APPENDIX A

Late Pleistocene regional extension rate derived from earthquake geology of late Quaternary faults across Great Basin, Nevada between 38.5° and 40° N latitude

Koehler, R.D. and Wesnousky, S.G. (in review)

In an effort to keep the guidebook brief I have shortened this paper that is currently in review. Text and figures related to ranges located to the east of this field trip have been removed. The appendix is also omitted. These data will be coming soon to a journal near you.

Late Pleistocene regional extension rate derived from earthquake geology of late Quaternary faults across Great Basin, Nevada between 38.5° and 40°N latitude

Rich D. Koehler and Steve G. Wesnousky (in review).
Center for Neotectonic Studies

ABSTRACT

Construction of maps showing Quaternary deposits and active fault traces, paleoseismic trenches, scarp diffusion analyses, and soil characteristics in displaced alluvial surfaces are combined with previous paleoseismic studies to examine the character of late Pleistocene earthquake recurrence and estimate the net extension rate across the interior of the Great Basin of the western United States at latitude of ~39°. The study area includes faults bounding the Desatoya, Toiyabe, Monitor, Simpson Park, Toquima, Antelope, Fish Creek, Butte, Egan, and Schell Creek Ranges. The rate of earthquake recurrence is documented to be significantly less than observed within the Walker Lane– Central Nevada Seismic Belt and along the Wasatch, which respectively define the western and eastern boundaries of the interior of the Great Basin. Late Pleistocene extension across the interior of the Basin is calculated to equal ~1 mm/yr across the 450 km transect and is consistent with rates defined by recent geodetic studies. The agreement in extension rate estimates over different time scales implies that relatively slow extensional deformation has been operative in the Great Basin east of the Central Nevada Seismic Belt through the late Pleistocene. From east to west the ranges become progressively more northeast trending and crustal velocities bend to the northwest. The organization of late Pleistocene ruptures into left stepping strands that trend oblique to rangefronts and are roughly perpendicular to N60W extension may be the geomorphic expression of a component of right lateral shear within the interior of the Great Basin.

INTRODUCTION

The internally drained high plateau between the Sierra Nevada in California and the Wasatch Mountains in Utah comprises the Great Basin section of the Basin and Range physiographic province (Figure 1A). The subparallel ranges and intervening basins are referred to as basin and range topography. The area is over 700 km wide and encompasses over two thirds of the ~1,000-km-wide Pacific/North American plate boundary. Geologic studies and modern space-based geodetic studies indicate that approximately 50 mm/yr of relative right-lateral deformation is distributed across the boundary (DeMets and Dixon, 1999). The majority of the deformation is localized along the San Andreas fault system in California (Savage et al., 2004; Freymueller et al., 1999). Approximately 15 - 25% is distributed east of the Sierra Nevada across the Great Basin

(Hammond and Thatcher, 2004; 2007; Bennett et al., 1998; 1999; 2003; Dixon et al., 1995; Minster and Jordan, 1987; Thatcher, 2003; Thatcher et al., 1999, Wernicke et al., 2000). The majority of the motion in the Great Basin is concentrated within the Walker Lane with a lesser amount of geodeticly-measured strain observed yet further east within the central and eastern Great Basin and the Wasatch Front (Figure 1A).

We here characterize the late Pleistocene rates of displacement and paleoseismic history of normal faults bounding ten mountain range fronts distributed across US HWY 50 including the Desatoya, Toiyabe, Toquima, Monitor, Simpson Park, Antelope, Fish Creek, Butte, Egan, and Schell Creek Ranges (Figure 1B). Information on the timing and amount of strain released by late Pleistocene earthquakes defines the manner in which contemporary strain across the region is ultimately accommodated by brittle deformation. Thus, the long-term geologic record of earthquake displacements and the relative age of faulted deposits are used to estimate a late Pleistocene extension rate. In this paper, we use the regional distribution of paleoearthquakes in time and space to make a first order comparison of the rate of strain release recorded by faulting to the rate of strain accumulation reported by geodecists elsewhere. We then discuss the map orientations of late Pleistocene ruptures in context to the eastern extent and direction of deformation associated with the northward propagation of the San Andreas fault along the Pacific/North American plate boundary.

BACKGROUND (GEOLOGY, GEODESY, EARTHQUAKE GEOLOGY)

Geologic Framework

The Pacific/North American plate boundary in the western United States is characterized by a broad diffuse zone of deformation distributed between the eastern front of the Basin and Range and the western continental shelf (Figure 1A)(Hamilton and Myers, 1966; Atwater, 1970; Minster and Jordan, 1987; Dixon et al., 1995; Bennett et al., 1999). Across present-day Nevada and Utah, the geographical distribution and structural development of mountain ranges reflects temporal changes in the style and rate of faulting from the Mesozoic to the present. Contractional orogenies related to the subduction of the Farallon Plate beneath North America during the Mesozoic resulted in a thickening of the continental crust in the Basin and Range of up to 50-60 km (Allmendinger, 1992; Coney and Harms, 1984). Processes considered to have contributed to crustal thickening include a flattening of the subducting Farallon plate, rapid subduction of a relatively young plate, and slab buoyancy forces (Dickinson and Snyder, 1979; Engebretson et al., 1985; Livaccari et al., 1981; Coney and Reynolds, 1977). An overprinting extensional regime was established in the Basin and Range by the late Paleogene and was associated with core complex formation along low angle detachment faults (Coney, 1987; Armstrong and Ward, 1991; Wernicke, 1992; Coney and Harms, 1984; Bartley et al., 1988; Taylor et al., 1989; Gans et al., 1989). The extensional deformation has been attributed to a combination of factors including a reduction in subduction rate, a change in plate motion convergent vector, and steepening or separation of the subducting plate (Engebretson et al., 1985; Humphreys, 1995), which caused high heat flow, lower crustal viscosity, and collapse of the gravitationally unstable

overthickened crust (Sonder and Jones, 1999; Coney, 1987; Coney and Harms, 1984; Sonder et al., 1987).

Extensional deformation within the Great Basin was influenced by plate boundary forces related to growth of the San Andreas fault system after Miocene subduction of the East Pacific Rise (Sonder and Jones, 1999; Atwater, 1970). High angle normal faults (block faulting) along predominantly north and northeast trending mountain ranges became the primary process controlling the modern physiographic expression of evenly spaced mountains and valleys in the Great Basin (Wallace 1984a; 1984b; Stewart, 1971; 1978; Gilbert, 1928) (Figure 1B). The structure is attributed to narrow zones of extension related to fragmentation of a brittle crust over a plastically extending substratum (Stewart, 1971). When combined with earlier low angle detachment faulting, the aggregate amount of extension is around150 km (Wernike, 1992; Coogan and DeCelles, 1996).

The physiographic expression of ranges across the region changes from north-south oriented ranges bounded by normal faults in the eastern Great Basin to progressively more northeast oriented ranges within the central Great Basin, where rangefront normal faults commonly diverge from the rangefront and extend into valleys in left stepping en echelon patterns. Northeast trending ranges abruptly terminate against northwest trending ranges along the eastern side of the Central Walker Lane (dark shaded area, Figure 1C). This abrupt boundary defines an overlapping transition between Basin and Range style extensional deformation to the north and east and transform deformation related to Pacific-North American relative plate motion to the southwest.

Geodetic Background

First order spatial and temporal patterns of strain accumulation across the western United States have now been defined by geodesy (Minster and Jordan, 1987; Argus and Gordon, 1991; Dixon et al., 1995; 2000; Hammond and Thatcher, 2004; 2007; Bennett et al., 1998; 1999; 2003; Thatcher et al., 1999; Thatcher 2003; Wernicke et al., 2000; Savage et al, 1995; Svarc, 2002b). Deformation in the Walker Lane is characterized by ~10 mm/yr of right-lateral shear parallel to the San Andreas. Deformation to the east from the CNSB to the Wasatch is dominated by easterly extension. Geodesy limits east-west extension rates < ~3mm/yr between the CNSB and Intermountain seismic Belt (IMSB) (Wernicke et al., 2000; Bennet et al., 1998; 2003; Hammond and Thatcher, 2007) with the majority of that (~1.6 mm/yr) focused along the Wasatch Fault Zone (Chang et al., 2006). Geodetic moment accumulation is closely correlated to seismic moment release rates across the Great Basin (Pancha et al., 2006).

Earthquake Geology

Paleoseismic investigations throughout the Great Basin including the Walker Lane, Central Nevada Seismic Belt, and Intermountain Seismic Belt have begun to elucidate long-term spacial and temporal patterns of earthquake recurrence particularly along the Basin margins. A summary of the paleoseismic histories reported in those

studies is provided in Table 1. We defer discussion of those results until later in the Discussion section where they are used to provide context for interpretation of the results we report here within the interior of the Basin. The methods employed to extract paleoearthquake information and the details of observation are presented in the next two sections. The reader interested in first examining the results may readily skip to the Discussion section.

METHODS

Fault Trenching

Structural, stratigraphic, and pedogenic relations exposed in natural exposures or trenches excavated normal to fault traces are the basis to place bounds on the paleoseismic history of faults at 8 sites within the study area. The approach is described in McCalpin (1996). Detailed stratigraphic unit descriptions for each trench are archived in Koehler (2009) and summarized in figure captions.

Scarp Profile Analysis

Fault scarp profiles were surveyed with a total station or by differential GPS to obtain measures of vertical displacement along each of the fault scarps investigated. The profile data was also used in diffusion analyses of fault scarp morphology to estimate the age of the earthquakes that produced the scarps, under the assumption that the initial scarp was produced by a single earthquake and morphology degrades systematically with time and initial scarp height (Bucknam and Andersen, 1979b; Wallace, 1977; Hanks and Wallace, 1985). The diffusion equation for scarps in Quaternary alluvium is written, $du/dt - \kappa(d^2u/dx^2) = 0$, where u is the relative elevation of a point on the scarp, which is a function, u(x,t), of the horizontal distance perpendicular to the scarp (x) and time (t), and κ is a diffusivity constant with units of m^2kyr^{-1} (Hanks, 2000; Hanks and Wallace, 1985). For faulted Quaternary deposits, where the initial slope is not flat, the solution to the diffusion equation is a function of the hanging and footwall slopes, the initial offset, κt, and an assumed value of friction (μ) that defines the initial angle of repose for a scarp in weakly consolidated materials (Hanks and Andrews, 1989). We use a value of friction ($\mu = 0.75$) and mass diffusivity ($\kappa = 1$) m^2kyr^{-1} and generate a synthetic profile that best fits the actual slope and offset of the measured scarp profile. The values of friction and diffusivity are consistent with those determined in diffusion studies of independently dated fault scarps in loosely consolidated alluvium and shoreline scarps of Lake Lahontan and Lake Boneville (Hanks, 2000; Hanks et al., 1984; Hanks and Wallace, 1985; Wesnousky et al., 2005). Curves are then generated for specific values of time keeping the other parameters constant until the synthetic profile visually best fits the surveyed profile. The result provides an estimate for the age of the earthquake that created the respective scarp. An example of the approach is shown in Figure 2 and a compilation of the synthetic and measured scarp profiles used in this study are compiled in (Appendix 1). The location of the profiles, estimated age for the earthquakes that created the scarps and the measured vertical separations are catalogued in Table 2 and used later to estimate the cumulative vertical and horizontal displacement across the transect (shown in Tables 3 and 4).

Surficial geologic mapping

Aerial reconnaissance of the study region was performed to identify surficial geologic map units and fault traces using (1) LandSat images, Digital Orthophotoquads (DOQ's), and Digital Elevation models (DEM's), (2) 1:60,000 scale black and white aerial photographs, (3)1:10,000 scale low sun angle black and white air photos, and (4) existing maps of fault traces and Quaternary deposits (Dohernwend et al., 1992; 1996; Haller et al., 2004; Schell, 1981). Field mapping was focused in areas most likely to preserve a record of fault displacements in late Quaternary deposits of various ages. Interpretation of geomorphic surfaces and the extent of fault scarps were field verified along each range and compiled on 1:24,000 scale 7.5' USGS topographic quadrangles.

Dating of alluvial surfaces and subsurface deposits

Geomorphic characteristics of the various map units are used to establish a relative stratigraphic chronology and evaluate the relative age of earthquake ruptures preserved in Quaternary alluvium across the HWY 50 transect. The chronology is based on surficial mapping and geomorphic principles used to differentiate and/or correlate alluvial units including relative degree of incision and rounding of surface morphology, cross cutting depositional and inset relations, amount of offset along fault scarps where progressively older surfaces are preserved at higher elevations, color, texture, and character of incision on air photos, and soil development. Highstand shoreline deposits associated with pluvial lakes provide a late Pleistocene time stratigraphic datum useful for relative age assessment throughout the region (Adams and Wesnousky, 1998; Miflin and Wheat, 1979; Reheis, 1999).

Soil formation is a function of time, climate, flora and fauna (biologic activity), parent material, and topography (Jenny, 1941). If all variables except time are relatively constant soil development progressively increases with time such that alluvial surfaces with more developed soils are older than surfaces with weaker soils. Specifically, the amount, thickness, and depth of B-horizon clay and pedgenic carbonate increases with age (Birkeland, 1999, Machette, 1985a). Carbonate accumulation in soils is related to the rate of leaching, the rate of weathering of calcium-bearing minerals, mean annual temperature (MAT), mean annual precipitation (MAP) and the carbonate content in rainfall, atmospheric dust, and parent materials (Birkeland, 1999; Machette 1985a). Although clast lithologies, temperature, and precipitation are slightly variable across the Great Basin, we make the simplifying assumption that changes in climate and carbonate available in the environment have been relatively similar across the HWY 50 transect and soils with similar carbonate stage development have similar relative age. Soils and carbonate stage development were described based on criteria outlined in Birkeland et al., 1991, Gile et al. (1966), Bachman and Machette (1977), Machette (1985b), and Birkeland (1999). Complete soil descriptions, laboratory clay percent vs. depth profiles, and mean annual temperature and precipitation data are archived in Koehler, 2009.

Carbonate stage development is used to place broad age constraints on displaced surfaces and maximum age estimates for the observed offsets. We draw on observations from previous studies that relate carbonate stage development to independent estimates of deposit age (Machette, 1982; Machette, 1985a; 1985b; McFadden, 1982; Harden and Taylor, 1983; Harden et al., 1991; 1985; Reheis, 1987; Treadwell-Steitz and McFadden, 2000; Taylor, 1989; Reheis and Sawyer, 1997; Sawyer, 1990; Slate, 1992; Reheis et al., 1995; 1996; McDonald et al., 2003; Kurth et al., in review). Combined, these studies indicate that soils that exhibit stage II to II+ carbonate development are late middle Pleistocene to late Pleistocene in age (~50-175 ka, as summarized in Redwine et al., in review).

The age of subsurface deposits that constrain the timing of earthquakes were determined based on tephra correlation (Sarna-Wojcicki and Davis, 1991), correlation with pluvial lake highstand deposits, and relative degree of soil development in strata buried by fault scarp colluvium (Birkeland, 1999). The lack of preservation of organic material in the arid alluvial deposits of the study area, limited the utility of radiocarbon dating. The results of the tephrochronology, radiocarbon, and bulk soil sieve analyses are recorded in Koehler (2009).

Quaternary Stratigraphy

Regionally generalized characteristics of individual geologic map units are depicted schematically in Figure 3. Detailed descriptions of sedimentological properties and air photo characteristics of each map unit are contained in Koehler (2009). Basin fill deposits (Qbf) represent a composite of deposits including those related to distal fan, pluvial lake, ephemeral stream, and aeolian processes. Quaternary to Holocene playa deposits (Hp) and lacustrine deposits (Ql) occur in the middle of basins, onlap pre latest Pleistocene alluvial fan deposits at basin margins, and locally, as playettes, flat areas behind highstand constructional deposits. Holocene dune deposits (Hd) form narrow discontinuous bands of loose sand and silt that fringe the edges of some basins. Latest Pleistocene alluvial fan deposits have incised and buried lacustrine deposits in upslope and downslope areas, respectively. Lacustrine beach deposits Q(bb) of paleo lakes form broad, flat, curvilinear bands with convex-up cross sectional morphology in map view. Well-preserved constructional landforms typically have thin, weakly developed soils similar to soils developed in latest Pleistocene deposits of the Sehoo highstand of pluvial Lake Lahontan (Adams and Wesnousky, 1999).

Young alluvial fan surfaces (Qfy) include active wash and alluvial fan deposits that are inset into pre latest Pleistocene alluvial surfaces. These surfaces originate in channels at the mountain front or within channels at the outboard edge of older elevated alluvial surfaces. Qfy deposits commonly extend to the valley floor, cut pluvial lake deposits, and interfinger with basin fill deposits. Small Qfy surfaces bury fault traces and older alluvial fan deposits along some rangefronts. Qfy surfaces are characterized by fresh bar and swale morphology, conical shape with a well-defined crest, and broad distributary drainage networks. Youthful morphology, weak soils that have stage I carbonate stage development (Birkeland, 1999), and cross cutting relations with pluvial

lake deposits, indicate that Qfy surfaces are latest Pleistocene to Holocene in age and generally post-date Lahontan age lake landforms.

Intermediate alluvial fans (Qfi) exist along rangefronts and also emanate from channels cut into remnant alluvial surfaces (Qfo). Qfy surfaces are deposited on and inset into Qfi surfaces in downslope and upslope areas, respectively. Qfi surfaces are inset 1-5 m into older alluvial surfaces and have been incised between 2-4 m by ephemeral streams. Lacustrine constructional features (Qbb) are deposited on Qfi surfaces and mimic the conical topographic shape of the underlying Qfi fan. Qfi surfaces are characterized by broad, flat relatively undissected morphology between stream channels, and a weak dendritic drainage pattern. Qfi deposits have moderately thick carbonate coatings on bioturbated clasts on the surface and moderately thick Bk soil horizons (20-40 cm) that have stage II to II+ carbonate stage development (Birkeland, 1999). Because Qfi deposits are buried by Lahontan age lacustrine landforms, the surfaces predate latest Pleistocene lacustrine deposits. Based on comparison to carbonate morphology developed in other soils in the region, Qfi surfaces may have been deposited between 50-175 ka (Redwine et al., in review). The similarity of clay percent profiles (Koehler, 2009) and carbonate development in soils developed in Qfi surfaces across the region suggests relatively synchronous deposition. The apparent sychroneity of Qfi deposits may be related to regional aggradation suggested by Eppes et al. (2003) to have occurred during intervals of climate change associated with marine oxygen isotope stages 4-3 (~70 kya) and 6-5 (~130 kya).

Old alluvial fan deposits (Qfo) occur as small, irregularly shaped landforms along rangefronts where the active fault steps across the piedmont slope. Large coalesced (Qfo) fan complexes that extend up to several km's into valleys are associated with rangefronts characterized by either long recurrence intervals or absence of active faulting. Isolated, backtilted Qfo remnants also occur along fault traces and grabens in mid valley areas. Qfo surfaces are characterized by smooth rounded morphology between drainages, well-developed dendritic drainage pattern, and deep incision (5-25+ m). Based on thick carbonate coatings on bioturbated clasts, multiple buried Btk horizons with stage III+ to IV carbonate stage development (Birkeland, 1999), and topographic position above Qfi surfaces, we infer that Qfo surfaces are middle Pleistocene or older in age.

Very old alluvial fan deposits and pediment surfaces (QTp) occur in isolated areas along some rangefronts. QTp surfaces/deposits have similar surficial characteristics to Qfo deposits with the exception of greater amounts of incision and rounding between stream interfluves. Active fault traces extend across the base of QTp surfaces and are responsible for their position and preservation. No exposures of soils developed into QTp surfaces were observed, however, based on their topographic position above Qfo deposits and geomorphic antiquity, QTp surfaces may have been abandoned in the early Pleistocene or Pliocene.

Across the region, each map unit exhibits similar sedimentologic, morphologic, and pedologic characteristics. These similarities may reflect regional climatic patterns that caused alternating periods of alluvial fan and pluvial lake development and periods

of relative incision and downcutting. Although temporally and spacially synchronous geomorphic processes may have occurred across the transect, determining the exact age of individual surfaces mapped as similar age (eg. Qfi) is problematic and may vary by several tens of thousands of years or more. Given these uncertainties, the regional stratigraphic framework is consistent throughout the study region and provides a means to compare relative rates of tectonic activity.

OBSERVATIONS

Observations bearing on general faulting characteristics are documented on a similar suite of Figures for each individual range. The Figures show: (1) The physiographic expression of the range, extent of previously mapped faults, and prominent landmarks; (2) the surficial expression of faults that cut Quaternary alluvium, both in air photos and field exposures; (3) Detailed field-based surficial geologic maps, focusing on areas most likely to preserve a record of late Quaternary displacements; and (4) profiles of fault scarps and sketches of subsurface relations exposed in trenches. The field observations are used to interpret the style, timing, and amount of deformation along each range and discussed separately below. The sum of observations are later used to estimate a long-term extension rate and examine regional deformation patterns.

Desatoya Range

Northwest flank, Desatoya Range

From southeast of Cold Springs to the vicinity of US Highway 50 the fault on the west side of the range is characterized by west dipping, left stepping normal faults that generally trend N10E to N20E along the bedrock alluvium contact (Figure 4). Our attention and mapping focused along the ~12-km long section of the fault shown in Figure 5 where the fault is characterized by subdued rangefront morphology, beveled scarps, overlapping, parallel, and left stepping strands, and progressively greater offsets of older alluvial fan surfaces. Here fault scarp heights are between 1.5 and 3 m and ~6 m in intermediate (Qfi) and old (Qfo) alluvial surfaces, respectively. Qfy surfaces have incised Qfi surfaces by several meters, eroded lacustrine deposits of pluvial Lake Edwards (Ql), and are not displaced by the fault. East of Edwards Creek, the fault steps south and becomes a less distinct, sinuous rangefront trace.

A photo and log of a trench excavated across the fault ~ 0.5 km west of the Edwards Creek channel where it produces a scarp in Qfi alluvium is shown in (Figure 6). The stratigraphy is interpreted to record three earthquakes along the western Desatoya Range fault. Unit 3 is fault scarp colluvium that accumulated against the scarp after Unit 1 was displaced and backtilted towards the fault by the first (oldest) earthquake. The colluvium (Unit 3) was exposed at the surface long enough for strong clay structure and carbonate nodules to develop. The penultimate earthquake is recorded by Unit 4, a colluvium deposited against the fault zone that buries Unit 3 and tapers away from the fault. The presence of Bt soil characteristics in the top of Unit 4 indicates exposure at the surface prior to burial by Unit 5. The separation of Units 3 and 4 from Unit 1 across an ~

1.5-m-wide shear zone characterized by vertically aligned clasts and the deposition of fault scarp colluvium across the fault zone (Unit 7) provides evidence for the most recent earthquake. The observations are consistent with surficial evidence for multiple earthquakes including beveled scarps and greater amount of offset along older deposits.

Because the scarp is the result of more than one earthquake, the site is not well suited for age determination by diffusion analyses. Scarp profiles (Profiles 1 and 2) surveyed across the fault at the site show a displacement of between 2.3 and 2.5 m, respectively (Table 2 and Appendix 1). All three earthquakes post-date the stage II carbonate soil developed in the Qfi alluvium (Unit 1). Inset geomorphic relations indicate that the earthquakes occurred prior to deposition of Qfy fans that cut the Qfi and lacustrine deposits. Undeformed lacustrine deposits where the fault crosses HWY 50 indicate that the last earthquake likely predates the late Pleistocene highstand of Lake Edwards. Thus, the three earthquakes occurred in the late Pleistocene with interevent times sufficient enough to develop soils on the two older colluviums. The lack of carbonate development in the most recent earthquake colluvium suggests that it occurred in the latest Pleistocence.

Southeast flank, Desatoya Range

The southeastern Desatoya rangefront consists of a southern and northern fault trace separated by an ~ 12 km left step across the vicinity of Smith Creek (Figure 4). The northern rangefront fault trace extends N30E for ~17 km from Smith Creek to Highway 50 (Figure 4). The tectonic geomorphic expression of the northern trace is subdued and characterized by rounded facets, low relief, and long shallow gradient alluvial fans. The muted topography and less developed rangefront morphology along the northern trace suggests a lower rate of fault displacements than the southern trace.

The southern trace extends ~ 20 km at N42E from Long Canyon to Stalefish Creek (Figure 4). Tectonic geomorphology along southern trace consists of a sharp linear rangefront with distinct oversteepened bedrock facets (>15 m high), several scarps in Qfi surfaces, and short steep alluvial fans (Qfy) that are actively burying Qfi surfaces and the fault trace (Figure 7). Prominent lacustrine constructional bar complexes and shoreline berms associated with pluvial Lake Desatoya are deposited on Qfi surfaces and cut by Qfy fans.

In the vicinity of Stalefish Creek, a 6-8 m high scarp in bedrock projects across a Qfi surface, which is offset a similar amount (Figure 7). The elevation of the scarp is slightly higher than the Lake Desatoya highstand shoreline elevation, but projects northeast into the basin where it has been covered by playette and prominent v-bar deposits (Figure 7). Three recessional berms associated with the v-bar have a slight northwest facing rise (scarp?) along strike with the fault. Because lacustrine features are not deformed further to the northeast along strike, it is unclear whether the rise is related to tectonic or lacustrine processes.

North of Stalefish Creek, the fault may continue on trend for another ~10 km based on a series of hot springs arranged along a linear rise (Figure 7). The rise consists of spring, aeolian, and lake deposits and is moister than the surrounding area. At the northern end of this linear rise, the position of the fault may coincide with anastamosing dark toned lineaments observed on air photos (Figure 7). In the field, the lineaments are characterized by groundwater seeps and aligned vegetation and do not exhibit vertical displacement. The observations support the occurrence of at least one late Pleistocene earthquake along the southern trace that occurred after the deposition of Qfi surfaces and prior to the highstand of Lake Desatoya.

Toiyabe Range

The north-northeast trending Toiyabe Range is one of the longest (~170 km) and most topographically prominent ranges in central Nevada (Figures 1B and 8). Topographic relief from the highest peaks to the valley floor is around 1800 m. The range is a west dipping horst block bound by active normal faults on both sides of the range. Each is described separately below.

East flank, Toiyabe Range

The fault trace is relatively continuous and commonly buried by colluvium and young alluvial fans along the bedrock escarpment. The escarpment is characterized by wineglass canyons, triangular facets, and oversteepened basal slopes (Figure 8). Scarps in Quaternary alluvium occur east of the rangefront along two approximately 5-km-long sections including an area south of Kingston Canyon and the area between Santa Fe Creek and Highway 50 (Figure 8). Detailed geologic mapping was conducted along the fault north of Santa Fe Creek and a trench was excavated across a fault scarp in Qfi alluvium directly north of Tar Creek (Figure 9).

A Qfi surface is displaced by two sub-parallel traces that extend ~N60E in the vicinity of the trench site (Figure 9). Scarps range from 1.5-2m and 2-3 m on the southeastern and northwestern traces, respectively. North of Lynch Creek, the northwestern trace projects along the base of a Qfo surface and is characterized by a sinuous 13-20 m high scarp and a possible 0.5 m splay scarp that trends N72E into a Qfi surface. Young alluvial fan surfaces (Qfy) associated with Tar Creek, Lynch Creek, and Spanish Canyon are not offset. North of Spanish Canyon the fault consists of two additional traces that step left towards the rangefront. The middle trace and upper trace offsets Qfo and Qfi surfaces by ~ 2 meters and a Qfo surface by over 20 m, respectively.

A trench excavated across the northwestern trace at Tar Creek exposed an offset package of alluvial fan gravels overlain by fault scarp colluvium (Figure 10). The history of faulting exposed in the trench supports the occurrence of two surface rupturing earthquakes that occurred after the deposition of the alluvial fan (Unit1). In the penultimate event, Unit 1 was down-dropped across the fault and Unit 2 (a block of Unit 1) was disrupted and back-tilted into a graben (Figure 10). Subsequent to the penultimate event, a fining upward eastward thinning package of scarp colluvium (Units 3 and 4) was

deposited against the free face. By projecting the top of Unit 1 on the hanging wall to the fault and measuring to the top of the penultimate colluvium, the penultimate event was associated with ~1.5 m of down to the south east displacement. The most recent event occurred after the deposition of Unit 4 based on separation of the penultimate colluvium from Unit 1 across the fault, and 0.5 to 1 cm thick carbonate lined shears extending through Units 2 and 3 that offset the base of Unit 4. Based on loose consistency, randomly oriented clasts, and some remnant bedding, Unit 6 is inferred to represent disrupted Unit 1 material that mixed with surface deposits as fissure fill during the most recent event. Unit 5 represents scarp derived colluvium associated with the most recent earthquake and consists of loose unconsolidated material and two, relatively hard blocks adjacent to the fault. The blocks are interpreted to be pieces of Unit 4 that rotated out of the fault zone during the most recent event. By measuring the vertical distance from the top of the penultimate colluvium to the top to Unit 1 on the footwall, the most recent earthquake was associated with about 0.5 m of normal displacement. Sufficient time has elapsed since the earthquake for erosional processes to mute the expression of the event on the surface.

Surface rupturing earthquakes recorded in the Tar Creek trench post-date the age of the Qfi deposit and associated soil cut by the fault. Soil descriptions at the site (Koehler, 2009) indicate that the hanging wall and footwall slopes comprise the same surface and are characterized by a 22 cm thick textural B horizon and stage II+ carbonate development (Birkeland, 1999). A scarp profile (Profile 1) surveyed adjacent to the trench shows a cumulative vertical separation for the two events of 1.8 m (Table 2). Therefore, the two events are broadly constrained to after late middle to late Pleistocene and after formation of the stage II+ carbonate soil developed in the Qfi fan. The comparatively less carbonate in the most recent event colluvium as compared to the penultimate colluvium, suggests a latest Pleistocene age for the most recent event.

West flank, Toiyabe Range

The western Toiyabe rangefront is a sharp linear escarpment characterized by large, well-developed, steep, triangular facets (Figure 8). Older generations of facets extend to the crest of the range and canyon mouths are typically deep, narrow, v-shaped knotches in bedrock that extend upwards into wineglass canyons. Between Highway 50 and Big Creek, large, steep, young alluvial fans are actively burying older alluvial surfaces along the rangefront and scarps in alluvium are not observed. Directly south of Big Creek an ~4-m-high fault scarp associated with a graben projects across an intermediate aged surface west of the rangefront (Figure 8). This scarp is beveled and likely represents more than one earthquake.

Simpson Park Range

The 72 km long Simpson Park Mountains extend between the Toquima Range and Cortez Range in the south and north, respectively, and is bounded on the west flank by a normal fault (Figures 2 and 11). Detailed surficial geologic maps illustrate the interaction of faulting and Quaternary deposits in the vicinity of Moonshine Canyon

(Figure 12) and adjacent to the Cortez Mountains (Figure 13). Along the southern part of the mapping area, between Moonshine Canyon and Walti Hot Springs the fault is a singular trace that follows a sawtooth pattern along the bedrock alluvial fan contact. The fault offsets Qfi and Qfo deposits in canyon salients with scarps up to 4 meters, and is expressed by well-defined facets, and prominent vegetation, spring, and bedrock lineaments. North of Walti Hot Springs, to the southern edge of the Cortez Mountains, the fault splits into at least three splays, becomes more sinuous, and displaces alluvial fans and pluvial landforms related to pluvial Lake Gilbert with scarps of 1 to greater than 10 meters. Between Walit Hot Springs and the Cortez Mounains, old alluvial fans are preserved adjacent to the rangefront, which is characterized by rounded and subdued facets. Along the Cortez Mountains, the fault is a singular trace where it is coincident with the highstand shoreline of Lake Gilbert for approximately 4 km before projecting uphill towards Mt Tenabu.

Trenches were excavated across the fault at two sites. Trench 1 is located across an ~2 m-high scarp that offsets the highstand shoreline of pluvial Lake Gilbert located ~4 km north of Walti Hot Springs (Figures 13). A log of the trench exposure is shown on Figure 14A. Stratigraphic and structural relations recorded in Trench 1 support the occurrence of two surface rupturing earthquakes that occurred after the deposition of Units 1 and 2. The occurrence of the penultimate event is supported by the juxtaposition of Units 1 and 2 against fault scarp colluvium (Unit 3) that accumulated against the scarp and sheared lenses of Units 1 and 2 within the 0.5-m-wide fault zone. The penultimate colluvium (Unit 3) was exposed at the surface long enough to accumulate pedogenic carbonate and become well-cemented. The penultimate paleoscarp was eroded by wave processes during the late Pleistocene transgression of pluvial Lake Gilbert, and was eventually buried by beach deposits (Unit 5). Subsequent to lake dessication, a soil developed on the beach gravels (Units 6 and7). Units 5, 6, and 7 extend across the entire exposure and are correlated across the fault where they are offset ~1.75 m and form a west facing scarp. The elevation of the soil on the footwall coincides with the 1750 m highstand elevation of pluvial Lake Gilbert (Miflin and Wheat, 1979, Reheis, 2002). The scarp, offset strata, fissure fills in Units 3 and 5, and fault scarp derived colluvium (Unit 8) that tapers away from the scarp are evidence for a second (most recent) paleoearthquake.

Trench 2 was excavated across an ~4 m high scarp in a young alluvial fan at the mouth of Pine Creek, ~6 km south of Walti Hot Springs along the rangefront (Figure 12). A sketch of the exposure is shown on Figure 14B. Structural and pedogenic relations observed in the trench supports the occurrence of one paleoearthquake that ruptured the surface after the deposition of Unit 1, creating an ~3-m-wide graben and an ~4 m high west facing scarp. Unit 2 is interpreted to represent graben fill material that toppled into the graben during the earthquake. During or shortly after the earthquake, a debris layer of colluvium (Unit 3) was deposited on the graben fill material. Subsequently, the hanging wall was buried by young alluvial deposits (Units 4, 5, 6, 7, and 10) and fault scarp derived colluvium (Unit 8).

The highstand shoreline of pluvial Lake Gilbert (1750 meters) is cut by the fault in several places (Figures 12 and 13) and correlated to the Trench 1 site by elevation. The timing of the highstand is inferred to be latest Pleistocene based on comparison of morphology and preservation of shore features to those of known Lahontan age (Mifflin and Wheat, 1979). Stratigraphic relations preserved in a gravel pit oriented oblique to the highstand beach berm in northern Grass Valley (Figure 14) indicate that the highstand predates the Mazama tephra (Koehler, 2009). Lake Lahontan reached its maximum extent at 13,070 +/- 60 14C BP (15,475 +/- 720 cal yr BP)(Adams and Wesnousky, 1999; Benson and Thompson, 1987a). Thus, the maximum limiting age for the most recent earthquake on the Simpson Park Mountains fault is latest Pleistocene.

Scarp Profile 1 surveyed adjacent to Trench 1 shows the surface offset is identical to the offset of the base of Unit 5 across the fault in the trench, indicating that the surface scarp was produced by a single earthquake (Table 2). The synthetic profile that best fits the observed profile is for an offset of 1.7 m and indicates the occurrence of an earthquake 6.5 kya (Table 2 and Appendix 1). At Trench 2, the diffusion analysis of Profile 2 places the offset at 4.2 meters and scarp formation at 9 ky a (Table 2 and Appendix 1). The two scarp profile ages for the most recent earthquake are consistent with the offset of latest Pleistocene lacustrine deposits of Lake Gilbert, and weak soil development in the footwall of trench 2. Considering that some time was necessary to develop a soil on the beach gravels at trench 1 (Units 6 and 7) prior to displacement, the age of the most recent earthquake is broadly constrained between latest Pleistocene and early Holocene. The close proximity and nearly continuous youthful scarps between the two trench sites suggests that the same earthquake is recorded at both sites. The penultimate event observed in Trench 1 occurred prior to the highstand of Lake Gilbert and prior to the accumulation of carbonate in the penultimate colluvium (Unit 3). Evidence for a penultimate event was not observed in trench 2, suggesting that it occurred prior to deposition of the fan or did not rupture as far south as the most recent event.

DISCUSSION AND CONCLUSIONS

Regional paleoseismic patterns and Extension Rate

A synopsis of the limits placed on the timing of surface rupturing earthquakes along each of the ranges studied is provided in Table 1. Information on the age of surface ruptures reported by others for faults in the Walker Lane and Central Nevada Seismic Belt and in Utah and used for context in this study are detailed in Koehler (2009), Wesnousky et al., (2005), and Hecker (1993). The history of paleoseismic displacements garnered in this study are combined with those of others in the form of a space-time diagram in Figure 15. The vertical axis is years and the horizontal axis is distance, expanded from the fault map of the northern Great Basin below. The solid lines in the underlying map mark the fault traces examined in this study. Faults studied by others are shown as gray lines or open boxes. Solid symbols in the overlying plot represent observations gathered in this study. The location of each symbol represents the age of an earthquake surface rupture. More specifically, circles indicate the age of earthquakes

determined from trench studies. In certain instances, stratigraphic and age constraints allow only the determination that a specific number of earthquakes have occurred subsequent to a particular age. In these cases solid squares are plotted and evenly divided over the age range. Stars indicate ages of earthquakes estimated by scarp diffusion analyses. Solid black vertical lines represent the range in age for a particular event. Dashed vertical lines indicate the approximate time interval for which observations are available. The earthquake histories for each fault on the space-time diagram are keyed to the map using number and letter labels. Collectively, the data represent a paleoseismic transect that spans the entire Great Basin from the Sierra Nevada to the Wasatch front, and is used to discuss the pattern of late Pleistocene strain release, as well as, the distribution and rate of occurrence of paleoearthquakes across the region.

Inspection of Figure 15 and Table 1 indicates that south of 40° N latitude a greater number of paleoearthquakes, and shorter recurrence intervals characterize the margins of the Great Basin, while fewer earthquakes, and longer recurrence intervals are typical for faults in the interior. For example, trench studies indicate at least 4 post ~15 ka earthquakes along the Pyramid Lake fault in the northern Walker Lane (Briggs and Wesnousky, 2004) and at least 3 Holocene events along the Nephi segment of the southern Wasatch Fault in the Intermountain Seismic Belt (Jackson, 1991; Schwartz et al., 1983). Trench studies in the interior of the Great Basin indicate recurrence intervals of several tens of thousands of years (Crone et al., 2006; Machette et al., 2005; Wesnousky et al., 2005). The observations are similar to the pattern of deformation documented geologically across the Great Basin north of the 40th parallel (Wesnousky et al., 2005) and geodetically across the region (Chang et al., 2006; Hammond and Thatcher, 2004; Kreemer et al., 2009; Thatcher et al., 1999; Bennet et al., 2003). The pattern is also consistent with dense seismicity within the Walker Lane, CNSB, and Intermountain Seismic Belt and diffuse seismicity within the interior of the Great Basin (Figure 1A) (Pancha et al., 2006; http://quake.geo.berkeley.edu/anss/catalog-search.html). Taken together, the spacial distribution of background seismicity and loci of increased geodetic strain are similarly reflected in the observation that the recurrence rate of surface rupturing earthquakes over the late Pleistocene is greater along the margins than within the interior of the Great Basin.

The observed late Pleistocene vertical displacements south of 40°N latitude provide a means to estimate the rate of extension between the Central Nevada Seismic Belt and the Wasatch Front. Displacements for the last ~60 ky and ~20 ky are catalogued in Tables 3 and 4, respectively. Horizontal displacement is estimated at each site based on assumptions attendant to the dip of the fault and the geometrical relation Tan(dip) = V.O./H.O., where V.O. is vertical offset and H.O. is horizontal offset. We assume a 60^0 dip for the faults at seismogenic depths in accordance with steep dips instrumentally recorded for historic earthquakes in the Great Basin (Doser, 1985; 1986) and frictional constraints associated with Andersonian mechanics (Anderson, 1951). To obtain a common east-west azimuth for each fault the calculated extension values are multiplied by the abs(cos(strike)) measured clockwise from north and recorded as HEW, (horizontal east-west extension). A net cumulative long-term extension rate across the ~500 km transect is estimated by summing the horizontal offsets and dividing by the time period

over which the offsets occurred, ~60 ky based on scarp diffusion. Displacements along the Wasatch fault, Walker Lane, and CNSB are omitted from the calculations to isolate deformation internal to the central Great Basin.

The earthquake displacements used in the extension rate calculation all post-date abandonment of their respective Qfi fan surfaces. The age of the Qfi fan surfaces provide a maximum age for the ruptures, and are used to independently verify the extension rate calculated using scarp diffusion ages for the ruptures. Based on regionally similar surface morphology, degree of incision, and soil development characterized by stage II to II+ carbonate development the Qfi surfaces are broadly constrained to between about 50-175 ky (Redwine et al., in review and references therein). This age range encompasses the timing of regional intervals of fan aggradation inferred to have occurred during marine isotope stage 4-3 (~70 ka) and 5-6 (~130 ka) (Eppes et al., 2003).

The total amount of measured vertical displacements between the CNSB and the Wasatch fault are 91.3 m and 35.4 m, over the last ~60 kyr and ~20 kyr, respectively (Tables 3 and 4). The calculated total net east-west horizontal extension over the same time periods is about 48.4 m and 19.3 m, respectively. Averaging these values over the time periods that the displacements occurred yields long-term extension rates of 48.4 m/60 kyr = 0.8 mm/yr and 19.3 m/20 kyr = 1.0 mm/yr. Dividing the total east west extension (48.4 m) by the possible range of ages for the displaced surfaces (50-175 ky) results in an extension rate of 0.3-1.0 mm/yr consistent with our result. Thus, a first-order estimate of the regional long-term extension rate across the Great Basin (0.8-1.0 mm/y r) is reasonable and has been operative over the late Pleistocene. The extension rate is similar to the rate determined for the area north of the 40th parallel (Wesnousky et al., 2005), suggesting that extensional strain release rates in the interior of the Basin are similar across the latitudes of 38.5°N to 41°N across the region.

The extension rate reported here encompasses geologic observations across the entire region but represents a minimum estimate. Unrecognized late Pleistocene slip may have occurred along rangefronts that have moderate tectonic geomorphology but lack scarps in alluvium including the eastern Shoshone, western Diamond, western White Pine, western Egan, and western Snake Ranges. However, if we account for the possiblility of 1 to 4 meters of slip on all of these ranges the extension rate only increases by ~0.2 mm/yr. An unknown amount of extension may be related to non-surface rupturing earthquakes, small scarps removed by erosion, fault traces within bedrock, and/or traces associated with half graben within valleys that are now buried by basin fill deposits. The analysis assumes that faults dip at 60° and displacements measured at the surface are representative of displacement at depth. The extension rate would be three times faster than our minimum estimate if the faults actually dip ~30°, however, this seems unlikely based on historical earthquake mechanisms that suggests steeper dips (Doser, 1985; 1986).

The Central Great Basin has previously been modeled as a rigid geodetic "microplate" extending east-west as a block with no significant internal deformation (Hammond and Thatcher, 2005; 2004; Thatcher et al., 1999; Bennett et al., 2003). This

was due primarily to the resolution and density of previous campain GPS studies. Recent geodetic modeling efforts incorporating results from high precision GPS data associated with the EarthScope array are beginning to better characterize crustal deformation in the region. In a study of the 21 February 2008 Mw 6.0 earthquake, Hammond et al. (in review) found a gradient in velocity of ~1mm/yr over a width of ~250 km across the interior of the Great Basin and a maximum horizontal crustal extension direction of N59W. Thus, withstanding the uncertainties, the long-term (geologic) net east-west extension rate of 0.8-1.0 mm/yr calculated here is, to first order, similar to short-term crustal velocities measured geodetically (Hammond et al., in review; Thatcher et al., 1999; Bennett et al., 2003).

Influence of the plate boundary on the late Pleistocene evolution of the Great Basin

The orientation of range crests and late Pleistocene ruptures are summarized on Figure 16. Stereo plots of rupture orientations for the areas east and west of the Diamond Range and a dextral strain ellipse approximately oriented parallel to the plate boundary are also shown on Figure 16. Across the width of the transect, the orientations of mountain ranges rotate from north-south orientations in the east to progressively more northeasterly trends to the west. East of the Diamond Range, late Pleistocene ruptures in alluvium primarily mimick the north-south trend of their respective ranges, and reflect east-west extension. Between the vicinity of the Diamond range and the Central Nevada Seismic Belt, late Pleistocene ruptures in alluvium are commonly oriented N25E to N55E, about 20° to 30° more northeast than their respective range crests. The geometry is consistent with northwest-directed extension and is expressed as northeast trending left stepping rupture patterns observed along most rangefronts. The regionally consistent orientation of the observed late Pleistocene ruptures suggest a response to a contemporary stress field that differs from the late Tertiary east-west extension that originally formed the topography.

Crustal deformation associated with the northward migration of the Mendocino Triple Junction through the latitude of this study over the last 6-8 my is characterized by northward propagation of the continuous northwest striking San Andreas fault system. The Walker Lane, ~250 km east of the San Andreas fault, has a more northerly trend than the plate motion vector, and is characterized by discontinuous northwest striking strike slip and normal faults connected across complex east striking left lateral faults. The less developed pattern of faulting within the Walker Lane as compared to the San Andreas fault, and widening of the northern Walker Lane has been attributed to a component of extension transverse to the trend of the Walker Lane, relatively less accumulated slip, and a transfer of northwest directed strike slip motion to northeast trending normal faults (Wesnousky, 2005; Hammond and Thatcher, 2005). In the Central Nevada Seismic Belt, historical earthquakes have been characterized by dextral, right oblique, and pure normal slip components, discontinuous left stepping north trending rupture patterns, and mole tracks (Gianella and Callaghan, 1934a; Bell et al., 1999; Caskey et al., 1996; 2004; Bell et al, 2004; Slemmons, 1956; Tocher, 1956). Thus, Pacific North American relative

motion is expressed by dominantly dextral motion in the Walker Lane and transitions to oblique deformation within the Central Nevada Seismic Belt.

East of the Central Nevada Seismic Belt, the orientation of range crests and late Pleistocene ruptures are consistent with geodetic displacement vectors that indicate ~N60W directed crustal extension (Hammond and Thatcher, 2007; Hammond et al., in review; Kreemer and Hammond, 2007). Figure 16 shows that faults in this orientation are optimally oriented to accommodate normal displacement in a right lateral plate boundary system. The northwest directed extension in the interior of the Great Basin along northeast trending normal faults is possibly the geomorphic expression of Pacific Plate motion. Old alluvial fan surfaces (Qfo) and Quaternary/Tertiary pediment surfaces are preserved along left stepping fault traces that trend oblique from rangefronts. Thus, the modern deformation field has been operative over at least the last several million years or longer, consistent with the timing of the migration of the Mendocino Triple Junction through the latitude of this study to the west. This suggests that the migration of the plate boundary may influence the pattern of Quaternary faulting over 200 km east of the Walker Lane.

ACKNOWLEDGEMENTS

This research was supported by National Science Foundation award EAR-0509672. Additional support to Koehler was provided by the Graduate Student Research Grants Program of the Geological Society of America and the Jonathan O. Davis Scholarship of the Desert Research Institute. Field assistance from the following is greatly appreciated: Humboldt State University field camp (2006; 2007), University of Nevada, Reno Quaternary mapping class (2005; 2006), Joanna Redwine, Jayne Bormann, Mark Hemphill-Haley, Jon Caskey, Paul Sundberg, and Jason Buck. Chuck Lane of the Bureau of Land Management, Battle Mountain District was invaluable in obtaining excavation permits. Center for Neoteconic Studies contribution # 54.

REFERENCES

Adams, K.D., and Wesnousky, S.G., 1999, The Lake Lahontan Highstand: age, surficial characteristics, soil development, and regional shoreline correlation: Geomorphology, v. 30, p. 357-392.

Adams, K.D., and Wesnousky, S.G., 1998, Shoreline processes and the age of the Lake Lahontan highstand in the Jessup embayment, Nevada: Geological Society of America Bulletin, v. 110, no. 10, p. 1318-1332.

Allmendinger, R.W., 1992, Fold and thrust tectonics of the western United States exclusive of the accreted terranes, In: The Cordilleran Orogen: Conterminous U.W., Burchfiel, B.C., Lipman, P.W., and Zoback, M.L. (Eds.), Geology of North America, vol. G3, Geologic Society of America, Boulder, Co., pp. 583-607.

Anderson, E. M. (1951), The Dynamics of Faulting, 206 pp., Oliver and Boyd, Edinburgh.

Anderson and Bucknam, 1979a, Map of fault scarps in unconsolidated sediments, Richfield 1^0 x 2^0 quadrangle, Utah, U.S. Geological Survey Open-File Report 79-1236, 15 p., scale 1:250,000.

Argus, D.F., and Gordon, R.G., 1991, Current Sierra Nevada-North America motion from very long baseline interferometry: Implications for the kinematics of the western United States,m Geology, v. 19, no. 11, p. 1085-1088.

Armstrong, R.L., and Ward, P., 1991, Evolving geographic patterns of Cenozoic magmatism in the North American Cordillera: The temporal and spatial association of magmatism and metamorphic core complexes, Journal of Geophysical Research, v. 96, no. B8, p. 13,201-13,224.

Atwater, T., 1970, Implication of plate tectonics for Cenozoic tectonic evolution for Western North America, Geological Society of America Bulletin, 81, p. 3513-3536.

Bachman, G.O., and Machette, M.N., 1977, Calcic soils and calcretes in the southwestern United States, U.S. Geological Survey Open-File Report 77-794, 163 p.

Bartley, J.M., Axen, G.J., Taylor, W.J., and Fryxell, J.E., 1988, Cenozoic tectonics of a transect through eastern Nevada near 38^0 north latitude, In: Weide, D.L., and Faber, M.L., edsl, This extended land, Geological journeys in the southern Basin and Range, Geological Society of America, Cordilleran Section, Field trip guidebook: Las Vegas, Nevada, Department of Geoscience, University of Nevada, p. 1-20.

Bell, J.W. and Katzer, T., 1990, Timing of late Quaternary faulting in the 1954 Dixie Valley earthquake area, central Nevada, Geology, 18, p. 622-625.

Bell, J. W., S. J. Caskey, A. R. Ramelli, and L. Guerrieri, 2004, Pattern and rates of faulting in the central Nevada seismic belt and paleoseismic evidence for prior belt-like behavior, Bulletin of the Seismological Society of America, 94, 1229– 1254, doi:10.1785/012003226.

Bell, J.W., dePolo, C.M., Ramelli, a.R., Sarna-Wojcicki, A.M., and Meyer, C.E., 1999, Surface faulting and paleoseismic history of the 1932 Cedar Mountain earthquake area, west-central Nevada, and implications for modern tectonics in the Walker Lane, Geological Society of America Bulletin, 111, p. 891-907.

Bennett, R.A., Wernicke, B.P., and Davis, J.L., 1998, Continuous GPS measurements of contemporary deformation across the northern Basin and Range province, Geophysical Research Letters, v.25, no. 4, p. 563-566.

Bennett, R.A., Wernicke, B.P., Niemi, N.A., Friedrich, A.M., and Davis, J.L., 2003, Contemporary strain rates in the northern Basin and Range province from GPS data, Tectonics, v. 22, no. 2, p. 1008.

Bennett, R.A., Davis, J.L., and Wernicke, B.P., 1999, Present-day pattern of Cordilleran deformation in the western United States, Geology, v. 24, no. 4, p. 371-374.

Benson, L.V., and Thompson, R.S., 1987a, Lake-level variation in the Lahontan basin for the last 50,000 years: Quaternary Research, v. 28,m p. 69-85.

Birkeland, P., Soils and Geomorhology, 432 pp., Oxford University Press, 1999.

Birkeland, P.W., Machette, M..N., and Haller, K.M., 1991, Soils as a tool for applied Quaternary geology, Manual for a short course, May 30-June 1, 1990, Utah Geological and Mineral Survey, Miscellaneous Publication Series.

Briggs, R. W., and S. G. Wesnousky, 2004, Late Pleistocene fault slip rate, earthquake recurrence, and recency of slip along the Pyramid Lake fault zone, northern Walker Lane, United States, J. Geophys. Res., 109, B08402, doi:10.1029/2003JB002717.

Bucknam, R.C., and R.E. Anderson, 1979b, Estimation of fault-scarp ages from a scarp-height-slope-angle relationship, Geology, 7, 11-14.

Bucknam and Anderson, 1979a, Map of fault scarps on unconsolidated sediments, Delta 10 x 20 quadrangle, Utah, U.S. Geological Survay Open-file Report 79-366, 21 p., scale 1:250,000.

Bucknam, R.C., Crone, A.J., and Machette, M.N., 1989, Characteristics of active faults, in Jacobson, J.L., ed., National Earthquake Hazards Reduction Program, summaries of technical reports volume XXVIII: U.S. Geological Survey Open-File Report 89-453, p. 117.

Caskey, J.S., Bell, J.W., Ramelli, A.R., and Wesnousky, S.G., 2003, Historic Surface Faulting and Paleoseismicity in the area of the 1954 Rainbow Mountain-Stillwater Earthquake Sequence, Central Nevada, Bulletin of the Seismological Society of America, resubmitted with revisions, Sept, 12, 2003.

Caskey, S. J., J. W. Bell, and S. G. Wesnousky, 2004, Historic surface faulting and paleoseismicity in the area of the

1954 Rainbow Mountain–Stillwater earthquake sequence, Bull. Seismol. Soc. Am., 94, 1255– 1275, doi:10.1785/012003012.

Caskey, S. J., J. W. Bell, D. B. Slemmons, and A. R. Ramelli, 2000, Historical surface faulting and paleoseismology of the central Nevada seismic belt, in Great Basin and Sierra Nevada, GSA Field Guide, vol. 2, edited by D. R. Lageson, S. G. Peters, and M. M. Lahren, pp. 23– 44, Geological Society of America, Boulder, Colo.

Caskey, S.J., Wesnousky, S.G., Zhang, P., and Slemmons, D.B., 1996, Surface faulting of the 1954 Fairview Peak (Ms 7.2) and Dixie Valley (Ms 6.8) earthquakes, central Nevada, Bulletin of the Seismological Society of America, v. 86, no. 3, p. 761-787.

Chang, Wu-Lung, Smith, R.B., Meertens, C.M., and Harris, R.A. 2006, contemporary deformation of the Wasatch Fault, Utah, from GPS measurements with implications for interseismic fault behavior and earthquake hazard: Observations and kinematic analysis, Journal of Geophysical Research, 111, B11405, doi:10.1029/2006JB004326.

Colman, S.M., and Watson, K., 1983, Ages estimated from a diffusion equation model for scarp degradation, Science, v. 221, no. 4607, p. 263-265.

Coney, P.J., and Reynolds, S.J., 1977, Cordilleran Benioff zones, Nature, v. 270, p. 403-406

Coney, P.J., 1987 The regional tetonic setting and possible causes of Cenozoic extension in the North American Cordillera, In: coward, M.P., dewey, J.F., and Hancock, P.L. (eds), 1987, continental Extensional Tectonics, Geological Society Special Publication No. 28, pp. 177-186.

Coney, P.J., and Harms, T.A., 1984 Cordilleran metamorphic core complexes: Cenozoic extensional relics of Mesozoic compression, Geology, v. 12, p. 550-554.

Coogan, J.C., and DeCelles, P.G., 1996, Extensional collapse along the Sevier Desert reflection, northern Sevier Desert basin, Western United States, Geology, vol. 24, no. 10, pp. 933-936.

Crone, A.J., 1983, Amount of displacement and estimated age of a Holocene surface faulting event, eastern Great Basin, Millard County, Utah, p. 49-55, In: Gurgel, K.D. (ed), 1983, Geologic Excursions in Neotectonics and Engineering Geology in Utah, Geological Society of America, Rocky Mountain and Cordilleran Sections Meeting, Salt Lake City, UT, Field Trip Guidebook, Part IV.

Crone, A.J., Kyung, J., Machette, M.N., Lidke, D.J., Okumura, K., and Mahan, S.A., 2006, Data related to late Quaternary surface faulting on the Eastgate Fault, Churchill County, Nevada, U.S. Geological Survey, Scientific Investigations Map 2893.

DeMets, C., and Dixon, T.H., 1999, New kinematic models for Pacific-North American motion from 3 ma to present: I Evidence for steady motion and biases in the NUVEL-1A model, Geophysical Research Letters, v. 26, p. 1921-1924.

dePolo, C. M., and Ramelli, A.R., 2003, The Warm Springs Valley fault system, A major rght-lateral fault of the northern Walker Lane, western Nevada, paper presented at XVI INQUA Congress: Paleoseismology in the Twenty-first Century, A Global Perspective, Session 19, Int. Union for Quat. Res., Reno, Nevada.

Dickinson, W.R. and W.S. Snyder, 1979, Geometry of subducted slabs related to San Andreas transform, Journal of Geology, 87, p. 609-627.

Dixon , T.H., Robaudo, S., Lee, J., and Reheis, M.C., 1995, Constraints on present-day Basin and Range deformation from space geodesy, Tectonics, 14 (4), p. 755-772.

Dixon, T.H., Miller, M., Farina, F., Wang, H., and Johnson, D., 2000, Present-day motion of the Sierra Nevada block and some tectonic implications for the Basin and Range Province, North American Cordillera, Tectonics, v. 1, p. 19-24.

Dohrenwend, J.C., Schell, B.A., and Moring B.C., 1992, Reconnaissance photogeologic map of young Faults in the Millett 1^0 by 2^0 Quadrangle, Nevada, U.S. Department of the Interior, U.S. Geological Survey, Miscellaneous Field Studies Map MF-2176.

Dohernwend, J.C., B.A. Schell, C.M. Menges, B.C. Moring, and M.A. McKittrick, 1996, Reconnaissance photogeologic map of young (Quaternary and Late Tertiary) faults in Nevada, Nevada Bureau of Mines and Geology Open-File Report, 96-2.

Doser, D. I., 1985, Source parameters and faulting processes of the 1959 Hebgen Lake, Montana, earthquake sequence, Journal of Geophysical Research, 90, 4537– 4555.

Doser, D. I., 1986, Earthquake processes in the Rainbow Mountain-Fairview Peak-Dixie Valley, Nevada, region 1954–1959, Journal of Geophysical Research, 91, 12,572– 12,586.

Eppes, M.C., McDonald, E.V., and McFadden, L.D., 2003, Soil geomorphological studies in the Mojave Desert: Impacts of Quaternary tectonics, climate, and rock type on soils, landscapes, and plant-community ecology, In: Easterbrook, D.J. (ed.), 2003, Quaternary Geology of the United States, INQUA 2003 Field Guide Volume.

Engebretson, D.C., Cox, A., and Gordon, R.G., 1985, relative motions between oceanic and continental plates in the Pacific Basin, Geological Society of America Special Paper 206, 59 p.

Freymueller, J.T., Murray, M..H., Segall, P., and Castillo, D., 1999, Kinematics of the Pacific-North America plate boundary zone, northern California, Journal of Geophysical Research, v. 104, p. 7419-7441.

Friedrich, A.M., Lee, J., Wernicke, B.P., and Sieh, K., 2004, Geologic context of geodetic data across a Basin and Renge normal fault, Crescent Valley, Nevada, Tectonics, 23, TC2015, doi: 10.1029/2003TC001528.

Gans, P.B., Mahood, G.A., and Schermer, E., 1989, Synextensional magmatism in the Basin and Range province: a case study from the eastern Great Basin, Geological Society of America Special Paper 233, 53 p.

Gianella, V.P., and Callahan, E., 1934a, The earthquake of December 20, 1932, at Cedar Mountain, Nevada, and its bearing on the genesis of Basin and Range structure, Journal of Geology, v. 42, no. 1, p. 1-22.

Gilbert, G.K., 1928, Studies of Basin and Range structure, U.S. Geological Survey Professional Paper 153, 1-92.

Gile, L.H., Peterson, F.F., and Grossman, R.B., 1966, Morphological and genetic sequences of carbonate accumulation in desert soils, Soil Science, v. 101, no. 5, p. 347-360.

Haller, K.M., Machette, M.N., Dart, R.L., and Rhea, B.S., 2004, U.S. Quaternary fault and fold database released, Eos, v. 85, no. 22, p. 218, U.S. Geological Survey, http://geohazards.cr.usgs.gov/qfaults/index.html.

Hamilton, W., and Myers, W.B., 1966, Cenozoic tectonics of the Western United States, Rev. Geophysics, v. 4, p. 509-536.

Hammond, W.C. and Thatcher, W., 2004, Contemporary tectonic deformation of the Basin and Range province, western United States: 10 years of observation with the Global Positioning System, Journal of Geophysical Research, vol. 109, B08403.

Hammond, W.C., and Thatcher, W., 2007, Crustal deformation across the Sierra Nevada, northern Walker Lane, Basin and Range transition, western United States measured with GPS, 2000-2004, Journal of Geophysical Research, vol. 112, B05411, doi: 10.1029/2006JB004625.

Hammond, W.C. and Thatcher, W., 2005, Northwest Basin and Range tectonic deformation observed with the Global Positioning System, 1999-2003, Journal of Geophysical Research, vol. 110, B10405, doi: 10.1029/2005JB003678

Hammond, W.C, Blewitt, G., Kreemer, C., Murray-Moraleda, J.R., and Svarc, J.L., in review, GPS constraints on crustal deformation before and during the 21 February 2008 Wells, Nevada M 6.0 Earthquake, NBMG/USGS 2008 Wells, Nevada Earthquake Report, submitted 13 November 2008.

Hanks, T.C., and Andrews, D.J., 1989, Effect of far-field slope on morphologic dating of scarplike landforms, Journal of Geophysical Research, v. 94, p. 565-573.

Hanks, T.C., and Wallace, R.E., 1985, Morphological analysis of the Lake Lahontan shoreline and beachfront fault scarps, Pershing County, Nevada, Bulletin of the Seismological Society of America, v. 75, p. 835-846.

Hanks, T.C., 2000, The age of scarplike landforms from diffusion-equation analysis, In: Noller, J.S., Sowers, J.M, and Lettis, W.R. (eds.), Quaternary Geochronology: Methods and Applications, Ref. Shelf, vol. 4AGU, Washington, D.C.

Hanks, T.C., Bucknam, r.C., Lajoie, K.R., and Wallace, R.E., 1984, Modification of wave-cut and faulting-controlled landforms, Journal of Geophysical Research, v. 89, no. B7, p. 5771-5790.

Harden, D.R., Biggar, N.E., and Gillam, M.L., 1985, Quaternary deposits and soils in and around Spanish Valley, Utah, In: Weide, D.L. (Ed.), 1985, Soils and Quaternary Geology of the Southwestern United States, Geological Society of America Special Paper 203.

Harden, J.W., and Taylor, E.M., 1983, A quantitative comparison of soil development in four climatic regions, Quaternary Research, v. 10, p. 342-359.

Harden, J.W., Taylor, E.M., Reheis, M.C., and McFadden, L.D., 1991, Calcic, Gypsic, and siliceous soil chronosequences in arid and semiarid environments, In: Occurrence, characteristics, and genesis of carbonate, gypsum, and silica accumulations in soils, Soil Science Society of America Special Publication no. 26.

Hecker, S., 1993, Quaternary Tectonics of Utah with Emphasis on Earthquake-Hazard Characterization, Bulletin 127, Utah Geological Survey, Utah Department of Natural Resources.

Humphreys, E.D., 1995, Post-Laramide removal of the Farallon slab, western United States, Geology, v. 23, no. 11, p. 987-990.

Hose, R.K. and Blake, M.C. Jr., 1976, Geology and Mineral Resources of White Pine County, Nevada, Nevada Bureau of Mines and Geology, Bulletin 85.

Jackson, M.E., 1991, Paleoseismology of Utah, volume 3-the number and timing of Holocene paleoseismic events on the Nephi and Levan segmentsm, Wasatch fault zone, Utah, Utah Geological Survey Special Studies 78, 23 p.

Jenny, H., 1941, Factors of Soil Formation, McGraw-Hill, New York.

Koehler, R.D., 2009, Late Pleistocene regional extension rate derived from earthquake geology of late Quaternary faults across Great Basin, Nevada between 38.5° and 40° N latitude, [Ph.D. thesis], University of Nevada, Reno.

Kreemer, C., Blewitt, G., Hammond, W.C., 2009, Geodetic constraints on contemporary deformation in the Northern Walker Lane: 2, Velocity and strain rate tensor analysis, *in* Late Cenozoic Structure and Evolution of the Great Basin – Sierra Nevada Transition, Geological Society of America Special Paper 447, p. 17-31, doi: 10.1130/2009.2447(03)

Kreemer, C., and Hammond, W.C., 2007, Geodetic constraints on areal changes in the Pacific-North American plate boundary zone: What controls Basin and Range extension, Geology, v. 35, no. 10, p. 943-947.

Kurth, G.E., Phillips, F., Reheis, M., Redwine, J.L., and Paces, J., (in review), Cosmogenic nuclide and uranium-series dating of old, high shorelines in the Western Great Basin, U.S.A., Geological Society of America Bulletin.

Livaccari, R.F., Burke, K., and Sengor, A.M.C., 1981, Was the Laramide orogeny related to subduction of an oceanic plateau, Nature, v. 289, p. 276-278.

Machette, M.N., Haller, K.M., Ruleman, C.A., Mahan, S.A., and Okumura, K., 2005, Geologic Evidence for late Quaternary movement on the Clan Alpine fault, west central Nevada- trench logs, scarp profiles, location maps, and sample and soil descriptions, U.S. Geological Survey, Scientific Investigations Map 2891, version 1.0.

Machette, M.N., Personius, S.F., and Nelson, A.R., 1992, Paleoseismology of the Wasatch Fault Zone: A Summary of Recent Investigations, Interpretations, and Conclusions, *In*: Assessment of Regional earthquake Hazards and Risk along the Wasatch Front, Utah, Gore, P.L. and Hays, W.W. (Eds.) U.S. Geological Survey Professional Paper 1500-A-J, 1992.

Machette, M.N., 1990, Temporal and spatial behavior of late Quaternary faulting, western United States, in Jacobson, J.L., ed., National Earthquake Hazards Reduction Program, Summaries of Technical Reports, volume XXXI: U.S. Geological Survey Open-File Report 90-680, p. 438-440.

Machette, M.N., 1985a, Calcic soils of the southwestern United States, In: Weide, D.L. (Ed.), 1985, Soils and Quaternary Geology of the Southwestern United States, Geological Society of America Special Paper 203.

Machette, M.N., 1985b, Late Cenozoic geology of the Beaver basin, southwestern Utah, Brigham Young University Geology Studies, v. 32, pt. 1, p. 19-37.

Machette, M.N., 1982, Guidebook to the late Cenozoic geology of the Beaver basin, south central Utah, U.S. Geological Survey Open-File Report82-850, 42 p.

McCalpin, J., Paleoseismology, 588 pp., Academic Press, New York, 1996.

McDonald, E.V., McFadden, L.D., and Wells, S.G., 2003, Regional response of alluvial fans to the Pleistocene-Holocene climatic transition, Mojave Desert, California, In: Enzel, Y., Wells, S.G., and Lancaster, N. (Eds.), Paleoenvironments and Paleohydrology of the Mojave and Southern Great Basin Deserts, Geological Society of America special paper no. 368, p. 189-205.

McFadden, L.D., 1982, The impacts of temporal and spacial climatic changes on alluvial soils genesis in southern California [PhD thesis], Tucson, University of Arizona, 430 p.

Mifflin, M.D. and Wheat, M.M., 1979, Pluvial lakes and estimated full pluvial climates of Nevada, Nevada Bureau of Mines and Geology Bulletin, 94, 57 pp.

Minster, J.B., and Jordan, T.H., 1987, Vector constraints on Western U.S. deformation from space geodesy, neotectonics, and plate motions, Journal of Geophysical Research, v. 92, p. 4798-4804.

Oviatt, C.G., 1989, Quaternary geology of part of the Sevier Desert, Millard County, Utah: Utah Geological and Mineral Survey Special Studies 70, 41 p., 1 pl., scale 1:100,000.

Oviatt, C.G., 1992, Quaternary geology of the Scipio Valley area, Millard and Juab Counties, Utah: Utah Geological Survey Special Studies 79, 16 p., scale 1:100,000.

Pancha, A., Anderson, J.G., and Kreemer, C., 2006, Comparison of Seismic and Geologic Scalar Moment Rates across the Basin and Range Province, Bulletin of the Seismological society of America, vol. 96, No. 1, pp. 11-32.

Piekarski, L.L., 1980, Relative age determination of Quaternary fault scarps along the southern Wasatch, Fish Springs, and House ranges, Brigham Young University Geology Studies, v. 27, pt. 2, p. 123-139.

Pierce, K.L., and Colman, S.M., 1986, Effect of height and orientation (microclimate) on geomorphic degradation rates and processes, late glacial terrace scarps in central Idaho, Geological Society of America Bulletin, v. 97, no. 7, p. 869-885.

Ramelli, A. R., Bell, J.W., dePolo, C. M., and Yount, J. C., 1999, Large magnitude,
late Holocene earthquakes on the Genoa fault, west-central Nevada and eastern California, Bull. Seismol. Soc. Am., 89, 1458–1472.

Ramelli, A. R., Bell, J. W., and dePolo, C.M., 2004, Peavine Peak: Another
piece of the Walker Lane puzzle, in Basin and Range Province: Seismic Hazards Summit, pp. 126– 127, Nev. Bur. of Mines and Geol., Reno, Nev.

Redwine, J., 2003, The Quaternary pluvial history and paleoclimate implications of Newark Valley, East-central Nevada; derived from mapping and interpretation of surficial units and geomorphic features, [Masters Thesis], Humboldt State University.

Redwine, J., Burke, R.M., Reheis, M.C., Bowers, R.J., Kaufman, D., Bright, J., Forester, R., and McGeehin, J., (in review), Middle to late Quaternary pluvial history of Newark Valley, east-central Nevada, Geological Society of America Bulletin

Reheis, M., 1999, Extent of Pleistocene lakes in the western Great Basin, U.S. Geological Survey Misc. Field Studies Map MF-2323, scale 1:800,000.

Reheis, M..C., 1987, Gypsic soils on the Kane alluvial fans, Big Horn County, Wyoming, U.S. Geological Survey Bulletin 1590-C, Soil Chronosequences in the Western United States.

Reheis, M.C., Slate, J.L., and Sawyer, T.L., 1995, Geologic map of late Cenozoic deposits and faults in parts of the Mt. Barcroft, Piper Peak, and Soldier Pass 15’ quadrangles, Esmeralda County, Nevada, and Mono County, California, U.S. Geological Survey Miscellaneous Investigations Series Map I-2264, scale 1:24,000.

Reheis, M.C., Slate, J.L., Throckmorton, C.K., McGeehin, J.P., Sarna-Wojcicki, A.M., and Dengler, L., 1996, Late Quaternary sedimentation on the Leidy Creek fan, Nevada-California, Geomorphic responses to climatic change, Basin Research, v. 12, p. 279-329.

Reheis, M.C., and Sawyer, T.L., 1997, Late Cenozoic history and slip rates of the Fish Lake Valley, Emigrant Peak, and Deep Springs fault zones, Nevada and California, Geological Society of America Bulletin, v. 109, no. 3, p. 280-299.

Sack, D., 1990, Geologic map of the Tule Valley, west-central Utah, Utah Geological and Mineral Survey Map 124, 26 p., pamphlet, scale 1:100,000.

Sarna-Wojcicki, A.M., and J.O. Davis, 1991, Quaternary tephrochronology, in Quaternary Nonglacial Geology: Conterminous U. S., edited by R.B. Morrison, pp. 93-116, Geological Society of America, Boulder.

Savage, J.C., Gan, W., Prescott, W.H., and Svarc, J.L., 2004, Stain accumulation across the Coast Ranges at the latitude of San Francisco, 1994-2000, Journal of Geophysical Research, B, Solid Earth and Planets, vol. 109, no. 3, 11 pp.

Savage, J. C., M. Lisowski, J. L. Svarc, and K. K. Gross, 1995, Strain accumulation across the central Nevada seismic zone, Journal of Geophysical Research, 100, 20,257– 20,269.

Sawyer, T.L., 1990, Quaternary geology and Neotectonic activity along the Fish Lake Valley fault zone, Nevada and California, [M.S. thesis], University of Nevada, Reno, 379 p.

Schell, B.A., 1981, Faults and lineaments in the MX Siting Region, Nevada and Utah, Volume II, Technical Report to the U.S. Department of Defense, Air Force, Norton Air Force Base, California, under Contract F04704-80-C-0006, 29 p., 11 pls., scale 1:250,000.

Schwartz, D.P., and Coppersmith, K.J., 1984, Fault behavior and characteristic earthquakes--Examples from the Wasatch and San Andreas fault zones: Journal of Geophysical Research, v. 89, no. B7, p. 5681-5698.

Schwartz, D.P., Hanson, K.L., and Swan, F.H., III, 1983, Paleoseismic investigations along the Wasatch fault zone-An update, In: Gurgel, K.D. (Ed.), Geologic excursions in neotectonics and engineering geology in Utah, guidebook-Part IV, Utah Geological and Mineral Survey Special Studies 62, p. 45-48.

Slate, J. L., 1992, Quaternary stratigraphy, geomorphology and geochronology of alluvial fans, Fish Lake Valley, Nevada–California [Ph.D. thesis]: Boulder, University of Colorado, 241 p.

Slemmons, D.B., 1956, Geologic setting for the Fallon-Stillwater earthquakes of 1954, Seismological Society of America Bulletin, v. 46, no. 1, p. 4-9.

Sonder, L.J., England, P.C., Wernicke, B.P., and Christiansen, R.L., 1987, A physical model for Cenozoic extension of western North America, Geological Society Special Publications, vol. 28, pp. 187-201.

Sonder, L.J., and Jones, C.H., 1999, Western United States Extension: How the West was Widened, Annu. Rev. Earth Planet. Sci, 27, p. 417-462.

Sterr, H.M., 1985, Rates of change and degradation of hill slopes formed in unconsolidated materials-a morphometric approach to dating Quaternary fault scarps in western Utah, USA, Zeitschrift fur Geomorphologie, v. 29, no. 3, p. 315-333.

Stewart, J.H., 1971, Basin and Range structure: A system of horsts and grabens produced by deep-seated extension, Geological Society of America Bulletin, v. 82, p. 1019-1044.

Stewart, J.H., 1978, Basin-Range Structure in western North America: a review, in Cenozoic Tectonics and Regional Geophysics of the Western Cordillera, R.B. Smith and E.P Eaton (editors), 1-32.

Svarc, J.L., Savage, J.C., Prescott, W.H., and Murray, M.H., 2002b, Stain accumulation and rotation in western Nevada, 1993-2000, Journal of Geophysical Research,m v. 107, doi:10.1029/2001JB000579.

Taylor, W.J., Bartley, J.M., Lux, D.R., and Axen, G.J., 1989, Timing of Tertiary extension in the Railroad Valley-Pioche transect, Nevada: Constraints from $^{40}Ar/^{39}Ar$ ages of volcanic rocks, Journal of Geophysical Research, v. 94, p.7,757-7,774.

Taylor, E.M., 1989, Impact of time and climate on Quaternary soils in the Yucca Mountain area of the Nevada Test Site, [M.S. thesis], University of Colorado, Boulder, Co.

Thatcher, W. (2003), GPS constraints on the kinematics of continental deformation, International Geology Review, 45, 191–212.

Thatcher, W., Foulger, G.R., Julian, B.R., Svarc, J.L., Quilty, E., and Bawden, G.W., 1999, Present-day deformation across the Basin and Range province, western United States, Science, v. 283, p. 1714-1718.

Tocher, D., 1956, Movement on the Rainbow Mountain fault, In: The Fallon-Stillwater earthquakes of July 6, 1954, seismological Society of America Bulletin, v 46., no 1, p. 10-14.

Treadwell-Steitz, C., and McFadden, L.D., 2000, Influence of parent material and grain size on carbonate coatings in gravelly soils, Palo Duro Wash, New Mexico, Geoderma, 94, p. 1-22.

Wallace, R.E. and Whitney, R.A., 1984, Late Quaternary history of the Stillwater seismic gap, Nevada, Bulletin of the Seismological Society of America, 74, 301-314.

Wallace, R.E., 1977, Profiles and ages of young fault scarps, north-central Nevada,
Geological Society of America Bulletin, 88, 1267-1281.

Wallace, R.E., 1984a, Fault scarps formed during the earthquakes of October 2, 1915, in Pleasant Valley, Nevada, and some tectonic implications, U.S. Geological Survey Professional Peper, 1274-A, A1-A33.

Wallace, R.E., 1984b, Patterns and timing of late Quaternary faulting in the Great Basin province and relation to some regional tectonic features, Journal of Geophysical Research, v. 89, p. 5763-5769.

Wernicke, B.P., Friedrich, A.M., Niemi, N.A., Bennett, R.A., and Davis, J.L., 2000, Dynamics of plate boundary fault systems from Basin and Range Geodetic Network (BARGEN) and geologic data, GSA Today, v. 10, no. 11, p. 1-7.

Wernicke, B.P., 1992, Cenozoic extensional tectonics of the Cordillera, U.S., In: Burchfiet, B., Lipman, P., and Zoback, M. (Eds.), The Geology of North America, vol. 63, The Cordilleran Orogen: Conterminous U.S.Geological society of America, Boulder, Colorado.

Wesnousky, S.G., Barron, A.D., Briggs, R.W., Caskey, J.S., Kumar, S., and Lewis, O., 2005, Paleoseismic Transect Across the Northern Great Basin, USA, Journal of Geophysical Research, Vol. 110, BO5408.

Wesnousky, S.G., 2005, Active faulting in the Walker Lane, Tectonics, 24, TC3009, doi:10.1029/2004TC001645.

Witkind, I.J., Weiss, M.P., and Brown, T.L., 1987, Geologic map of the Manti 30’ x 60’ quadrangle, Carbon, Emery, Juab, Sanpete, and Sevier Counties, Utah: U.S. Geological Survey Miscellaneous Investigations Map I-1631, scale 1:100,000.

Table 1. Paleoseismic summary for faults in Nevada and Utah between 38.5° and 40° North latitude. Fault numbers correlate to faults on Figure 15. Information for faults shown on Figure 15 that are north of 40° N latitude is contained in Wesnousky et al. (2005) and Koehler (2009).

Fault[a]	Number and timing of events[b], and slip rate	Reference[c]
2. Peavine Peak	4-5 events in last 6,000-8,000 yrs	a
4. Warm Springs	At least 3 events in latest Pleistocene	E
5. Pyramid Lake	at least 4 events post ~15,500 cal yrs BP; MRE after 1,705 ± 175 cal yrs BP	c
1.Genoa	2 events,500-600 cal yrs BP; 2,000-2,200 cal yrs BP	b
D. 1954 Rainbow-Stillwater	3 events: 1954 AD; 6.3-9.9 ka; 8.1-17.8 ka; plus event at 0.0-1.5 ka on Fourmile Flat strand. Slip rate 0.4 mm/yr; post latest Pleistocene slip rate 0.2-0.46 mm/yr	de
C. 1954 Dixie Valley	3 events: 1954 AD; 2.0-2.5 ka; <35 ka	fe
B. 1954 Fairview Peak	2 events: 1954 AD; >35 ka	ge
A. 1932 Cedar Mt.	6 events: 1932 AD; 4 ± 2 ka; 5 ± 2 ka; 12 ± 2 ka; 15 ± 2ka; 18 ± 2 ka	h
14. Desatoya (W)	3 late Pleistocene events[d] ; MRE latest Pleistocene <20ka? +/-10[de]	i
15. Desatoya (E)	At least 1 late Pleistocene event, predates highstand of Lake Desatoya	i
12. Eastgate	3 events in last 28 ka, MRE before 4.4 ka; penultimate ~17 ka	G
13. Clan Alpine	2 or 3 events post ~130 ka; MRE before 9 ± 1 ka; penultimate before 28 ± 3 ka	j
16. Toiyabe (W)	At least 2 late Pleistocene events based on beveled 4-m-high scarp	i
18. Toiyabe (E)	2 events in late Pleistocene[e], MRE latest Pleistocene	i
23. Toquima	Southern part, at least1 event: ~55-60 ka[f], Northern part (Hickison Summit area), at least 1 event ~16 ka[f]	i
22. Simpson Park	2 events: MRE 6-9 ka[f] and post ~15,500 cal yrs BP; penultimate pre Lake Gilbert highstand	i
24. Monitor (W)	1 event: ~44 ka[f]	i
Monitor (E)	At least 1 late Pleistocene event[g]	i
25. Antelope	2 events: ~15-21 ka[f]; ~44-66 ka[f]	i
26. Fish Creek	1 event: ~28-29.7 ka[f]	i
27. Diamond Range (E)	At least 1 late Pleistocene event, predates highstand of Lake Newark[g]	i, F
28. Butte	3 late Pleistocene events: MRE ~18-25 ka[f]; 2 older events	i
31. Egan (E)	1-2 events: ~21-36 (?) ka[f]; ~60 ka[f]	i
36. Schell Creek	2-3 late Pleistocene events: 1-2 events between ~10-30 ka[f] and 1 older event	i
33. Snake Valley	At least 1 event <15 ka, 2.4 m displacement	oH
34. Deep Creek Range (E)	At least 1 event, middle to late Pleistocene, scarps ~13 m	oH
36. House Range	At least 1 event: ~12-19 ka[f] and post Bonneville transgression	lm
35. Fish Springs	4 events post Bonneville highstand: MRE ~2 ^{14}C ka-4.8 ka[f]	nopqr
37. Crickett Mt.	at least 2 events: MRE post Provo shoreline; penultimate pre Bonneville	sto
38. Drum Mt.	at least 2 events: MRE between ~12 ka[f] and early Holocene; penultimate pre Bonneville	ouvwq x
39. Clear Lake	1 event: Holocene	vt

Table 1. Continued.

44. Little/Scipio V.	Red Canyoun scarps: surface displacement of 2.2 m in latest Pleistocene to Holocene; Maple Grove fault: cumulative displacement of 12 m, late Pleistocene predating Boneville highstand; Pavant Range fault: at least 1 Holocene event; Scipio Valley fault: cumulative late Pleistocene displacement of 11 m and 1 late Holocene event with 2.7 m displacement; Little Valley fault, cumulative displacement of 8.2 m, late Pleistocene predating Boneville highstand.	ovy
45. Japanese V.	At least 1 event, offset 4 m, late Pleistocene to Holocene	tz
47. Southern Wasatch	Nephi segment; MRE after 1,350 ± 70 ^{14}C yrs BP, penultimate before 3,841 cal yr BP; oldest after 5,300 ± 300 ka. Levan segment: 2 events: MRE after ~2 ka multiple dates; penultimate before 3.1 ka. Fayette segment: at least 1 event ~10-15 ka[f]	ABCD

[a] (W) or (E) indicates west or east side of range. Southern Wasatch includes Nephi, Levan, and Fayette segments.
[b] Surface rupture. Uncorrected ages in thousands of years listed as ka; calibrated radiocarbon ages listed as cal yr BP; MRE most recent earthquake.
[c] References: a, Ramelli et al. (2004); b, Ramelli et al. (1999); c, Briggs and Wesnousky, 2004; d, Caskey et al. (2004); e, Bell et al. (2004); f, Bell and Katzer (1990); g, Caskey et al. (2000); h, Bell et al. (1999); i, this study; j, Machette et al. (2005); k, Friedrich et al. (2004); l, Piekarski (1980); m, Sack (1990); n, Machette (1990); o, Hecker (1993); p, Bucknam et al. (1989); q, Hanks et al. (1984); r, Sterr (1985); s, Anderson and Bucknam (1979a); t, Oviatt (1989); u, Crone (1983); v, Bucknam and Anderson (1979a, 1979b); w, Colman and Watson (1983); x, Pierce and Colman (1986); y, Oviatt (1992); z, Witkind et al., 1987; A, Jackson (1991); B, Schwartz et al (1983); C. Schwartz and Coppersmith (1984); D, Machette et al. (1992); E, dePolo and Ramelli (2003); F. Redwine (2003); G, Crone et al. (2006); H, Schell (1981).
[d] observations from trench and soils.
[e] based on carbonate development in offset fan.
[f] Best estimate from fault scarp profiling. Uncertainty ~ 10 ky.

Table 2. Vertical separation measured from fault scarp profiles and best estimate of scarp age based on diffusion analysis. Diffusion analyses assume a value of friction ($\mu = 0.75$) and mass diffusivity ($\kappa = 1$) m^2kyr^{-1}. Age estimates are not provided for scarps determined to be related to multiple events. Coordinates for each profile are in WGS84 projection.

Range	Profile name	Easting	Northing	Vertical displacement	Estimate of scarp age
Desatoya	Profile 1	436060.5625	4370546.5	2.3	N.A.
	Profile 2	436079.03125	4370557.0	2.5	N.A.
Toiyabe	Profile 1	498115.5	4353974.77	1.8	N.A.
Simpson Park	Profile 1	536419.4131	4421281.38	1.7	6.5
	Profile 2	535605.25	4410974.0	4.2	9
Toquima	Profile 1	515296.0625	4300354.0	1.87	55
	Profile 2	525610.4375	4320799.5	1.1	60
	Profile 3	526196.375	4374000.0	1.1	16
Monitor	Profile 1	532403.75	4350846.0	0.85	44
	Profile 2	532385.5	4350775.0	0.85	44
Antelope	Profile 1	561383.125	4338642.5	3.7	N.A.
	Profile 2	562414.625	4340731.5	3.0	N.A.
	Profile 3	570345.313	4354190.5	1.7	21
	Profile 4	570330.1875	4354168.5	1.6	15
Fish Creek	Profile 1	580752.8125	4346358.0	2.7	29.7
	Profile 2	580736.3125	4346351.0	2.3	28
Butte	Profile 1	645689.5	4403714.5	0.95	18
	Profile 2	645691.375	4403705.0	1.3	22
	Profile 3*	643470.4856	4399653.5	4.2	22
	Profile 4*	643470.4856	4399653.5	4.4	25
	Profile 5	642651.875	4397001.5	5.3	N.A.
Egan	Profile 1	686397.875	4394087.5	1.3	42
	Profile 2	686394.4375	4394098.5	1.3	60
	Profile 3	681015.4375	4383295.0	2.2	N.A.
	Profile 4	681010.1875	4383286.5	1.6	N.A.
Schell Creek	Profile 1	713815.875	4343132.0	1.04	N.A.
	Profile 2	713815.75	4343135.5	0.98	N.A.
	Profile 3	713450.875	4343035.0	0.84	N.A.
	Profile 4	713447.25	4343040.0	0.77	N.A.
	Profile 5	711908.625	4374068.0	3.85	30
	Profile 6	711912.75	4374018.0	3.7	35
	Profile 7	711917.75	4373988.0	3.6	32

* Coordinates for Profiles 3 and 4 along the Butte Range are actually the coordinates of the trench. The profiles were surveyed ~4 m north and south of the trench.

Table 3. Earthquake displacements for last ~ 60 ky. Estimate does not include rangefronts with prominent tectonic geomorphology where alluvial surfaces are not offset. Fault numbers correlate to faults on Figure 57.

Fault[a]	Vertical Separation[b]	Extension	Strike	HEW
13. Clan Alpine (E)	6[t]	3.5	27	3.1
12. Eastgate (W)	6.9[t]	4	327	3.3
14. Desatoya (W)	2.5[p]	1.4	50	0.9
15. Desatoya (E)	6[f]	3.5	32	2.9
23. Toquima North (Hickison Summit) (E)	1.1 [p]	0.6	35	0.5
22. Simpson Park (W)	4.2 [p]	2.4	35	2.0
16. Toiyabe (E)[c]	3.3 [pf]	1.9	32	1.6
18. Toiyabe (W)	4.0[f]	2.3	29	2.0
23. Toquima South (E)	3.0 [p]	1.1	32	0.9
48. Monitor (E)	2[f]	1.2	45	0.8
24. Monitor (W)[d]	1.7 [pf]	1.0	15	0.9
25. Antelope (W)	3.7 [p]	2.1	27	1.9
26. Fish Creek (E)	2.7 [p]	1.6	15	1.5
27. Diamond (E)	3[f]	2.3	0	2.3
28. Butte (W)	5.3 [p]	3.1	10	3.0
31. Egan (E)	2.2 [p]	1.3	15	1.2
32. Shell Creek (E)	3.85 [p]	2.3	0	2.3
33. Snake Valley (E)	2.4	1.4	0	1.4
34. Deep Creek (E)	?	?	20	?
35. Fish Springs (E)	3.3[p]	1.9	358	1.9
36. House (W)	1.4[f]	0.8	0	0.8
37. Crickett Mts. (W)	1.3[f]	0.8	17	0.7
38. Drum Mts. (E)	2.4[ft]	1.4	353	1.4
39. Clear Lake (E)	3[f]	1.7	351	1.7
44. Little/Scipio Valley (E)	12[f]	6.9	0	6.9
45. Japanese/Cal Valley (W)	4[f]	2.3	4	2.3
SUM	91.3	58.5		48.4

Extension Rate = 48.4 m/60 ka = 0.8 mm/yr

[a] Fault dip direction indicated by E (east) and W (west). Fault number corresponds to faults on Figure 15.
[b] Method used to estimate vertical separation. t, interpreted from trench exposure; p, scarp profile; f, field measurement with hand level or previously reported height from field mapping studies. References for each fault are the same as those reported in Table 1.
[c] Scarp profile measurement combined with hand level scarp height of secondary scarp to estimate total separation.
[d] Total separation estimated by combining scarp profile measurement and height of a similar scarp upslope.

Table 4. Earthquake displacements for last ~ 20 ky. Estimate does not include rangefronts with prominent tectonic geomorphology where alluvial surfaces are not offset. Fault numbers correlate to faults on Figure 15.

Fault[a]	Vertical Separation[b]	Extension	Strike	HEW
13. Clan Alpine (E)	1.2[t]	0.7	27	0.6
12. Eastgate (W)	1[t]	0.6	327	0.5
14. Desatoya (W)	0.8[t]	0.5	50	0.3
23. Toquima North (Hickison Summit) (E)	1.1[p]	0.6	35	0.5
22. Simpson Park (W)	4.2[p]	2.4	35	2.0
18. Toiyabe (E)	0.4[t]	0.2	32	0.2
25. Antelope (W)	1.7[p]	1.0	27	0.9
28. Butte (W)	1.3[p]	0.8	10	0.7
32. Shell Creek (E)	1.9[p]	1.4	0	1.4
33. Snake Valley (E)	2.4	1.4	5	1.4
35. Fish Springs (E)	3.3[p]	1.9	358	1.9
36. House (W)	1.4[f]	0.8	0	0.8
37. Crickett Mts. (W)	1.3[f]	0.8	17	0.7
38. Drum Mts. (E)	3.7[ft]	2.1	353	2.1
39. Clear Lake (E)	3[f]	1.7	351	1.7
44. Little/Scipio Valley (E)	2.7[f]	1.6	0	1.6
45. Japanese/Cal Valley (W)	4[f]	2.3	4	2.3
SUM	35.4	24.5		19.3

Extension Rate = 19.3 m/20 ka = 1.0 mm/yr

[a] Fault dip direction indicated by E (east) and W (west). Fault number corresponds to faults on Figure 15.
[b] Method used to estimate vertical separation. t, interpreted from trench exposure; p, scarp profile; f, field measurement with hand level or previously reported height from field mapping studies; w, thickness of colluvial wedge. References for each fault are the same as those reported in Table 1.

Figure 1. (A) Active faults and seismicity of the Pacific-North American plate boundary in western United States. Faults shown by black lines, seismicity shown by black dots, Major tectonic elements of the Great Basin are also labeled. Seismicity is M>2 (since 1944) from Advanced National Seismic System's catalog (http://quake.geo.berkeley.edu/anss/catalog-search.html). Faults from Dohernwend et al. (1996) and the Fault and Fold Database of the U.S. Geological Survey (Haller et al., 2004: http://qfaults.cr.usgs.gov). Plate motion velocity vector from DeMets and Dixon, 1999. Approximate boundaries of provinces within the Great Basin taken from Bennett et al. (2003). (B) Location of normal fault bounded mountain ranges within the Great Basin that are the focus of this study. Also indicated are mountain ranges referred to in the text. Faults taken from the Fault and Fold Database of the U.S. Geological Survey (Haller et al., 2004: http://qfaults.cr.usgs.gov). White stars are permanent GPS monuments recently installed as part of the Earthscope element of the Plate Boundary Observatory project. US Highway 50 and Highway 6 shown in black. EF, East Gate fault; CA, Clan Alpine Range; DES, Desatoya Range; TOI, Toiyabe Range; TOQ, Toquima Range; SP, Simpson Park Range; M, Monitor Range; A, Antelope Range; FC, Fish Creek Range; D, Diamond Range; P, Pancake Range; WP, White Pine Range; G, Grant Range; B, Butte Range; E, Egan Range; SE, South Egan Range; SC, Schell Creek Range; S, Snake Range. (C) Location map for faults of the central (shaded dark gray) and northern (shaded light gray) Walker Lane and Central Nevada Seismic Belt (CNSB) discussed in text. HL, Honey Lake fault; WS, Warm Springs fault; PL, Pyramid Lake fault; OH, Olinghouse fault; MV, Mohawk Valley fault; MR, Mount Rose fault zone; IV, Incline Village fault; ET, East Tahoe fault; WTDP, West Tahoe Dollar Point fault; CCF, Carson City fault; CL, Carson Lineament; WL, Wabuska Lineament; GF, Genoa fault; AV, Antelope Valley fault; SV, Smith Valley fault; WR, Wassuk Rangefront fault; HV, Huntoon Valley fault; EM, Excelsior Mountains fault; RF, Rattlesnake Flat fault; IH, Indian Head fault; BS, Benton Springs fault; GH, Gumdrop Hills fault; PS, Petrified Springs fault; FF, Fourmile Flat fault; RM, Rainbow Mountain fault; FP, Fairview Peak fault; DV, Dixie Valley fault; PV, Pleasant Valley fault; EG, Eastgate fault; CA, Clan Alpine fault; WD, West Desatoya fault; ED, East Desatoya fault; SR, Singatse Range fault; KC, Kings Canyon fault zone; CH, Candelaria Hills fault; MCV, Monte Cristo Valley fault zone; GV, Gabbs Valley.

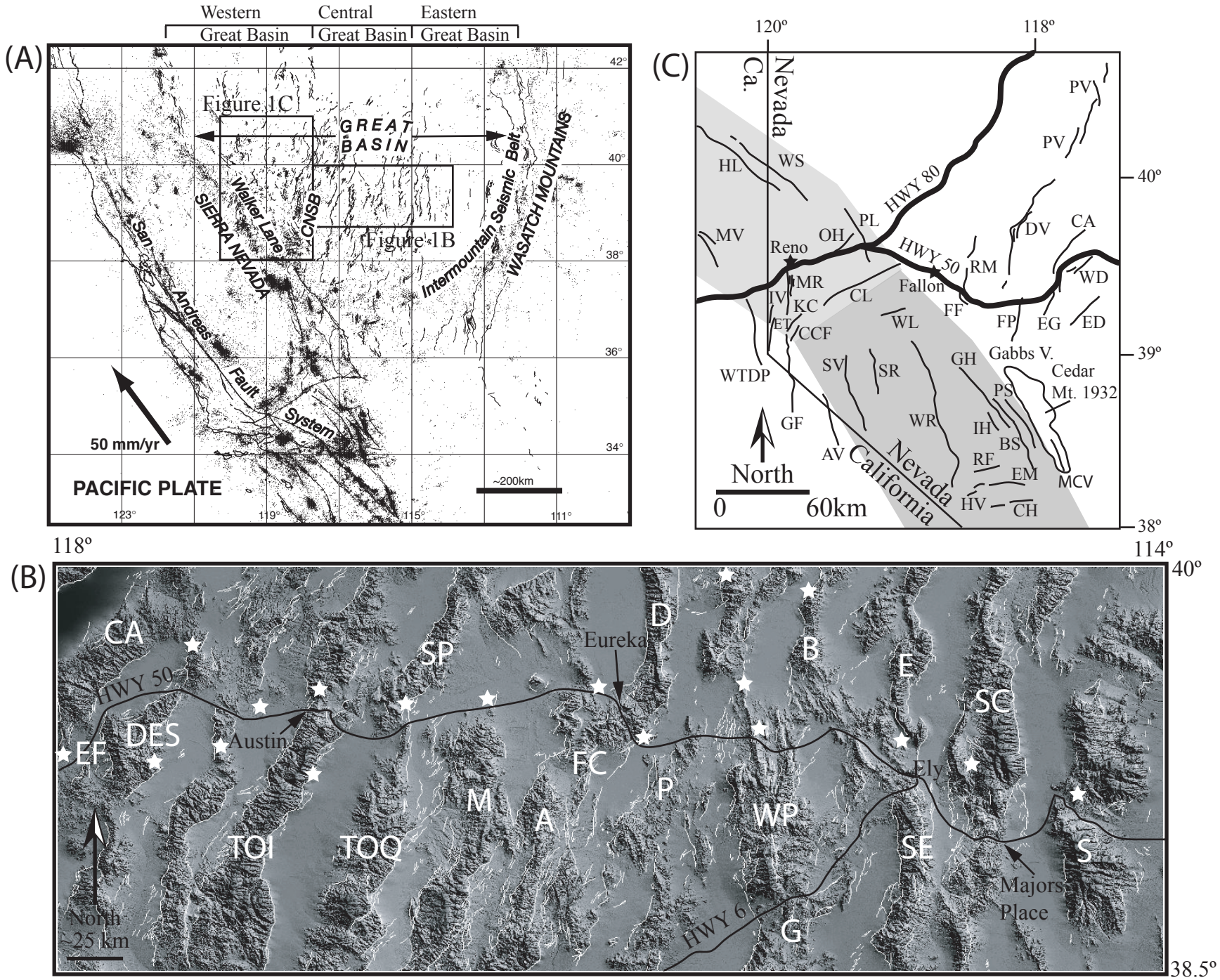
(A)
Western Great Basin
Central Great Basin
Eastern Great Basin
Figure 1C
GREAT BASIN
Walker Lane
CNSB
SIERRA NEVADA
Figure 1B
Intermountain Seismic Belt
WASATCH MOUNTAINS
San Andreas Fault System
50 mm/yr
PACIFIC PLATE
~200km
42°
40°
38°
36°
34°
123°
119°
115°
111°
118°
(C)
120°
118°
Ca.
Nevada
PV
PV
HL
WS
HWY 80
40°
MV
OH
PL
DV
CA
Reno
HWY 50
RM
WD
MR
Fallon
IV
KC
CL
FF
ET
CCF
WL
FP
EG
ED
Gabbs V.
39°
WTDP
SV
SR
GH
Cedar
Mt. 1932
PS
GF
WR
IH
BS
AV
California
Nevada
RF
EM
MCV
North
0
60km
HV
CH
38°
114°
(B)
40°
CA
HWY 50
SP
D
Eureka
B
E
SC
EF
DES
Austin
FC
Ely
M
P
WP
A
TOI
TOQ
SE
S
Majors Place
North
~25 km
HWY 6
G
38.5°

Figure 1.

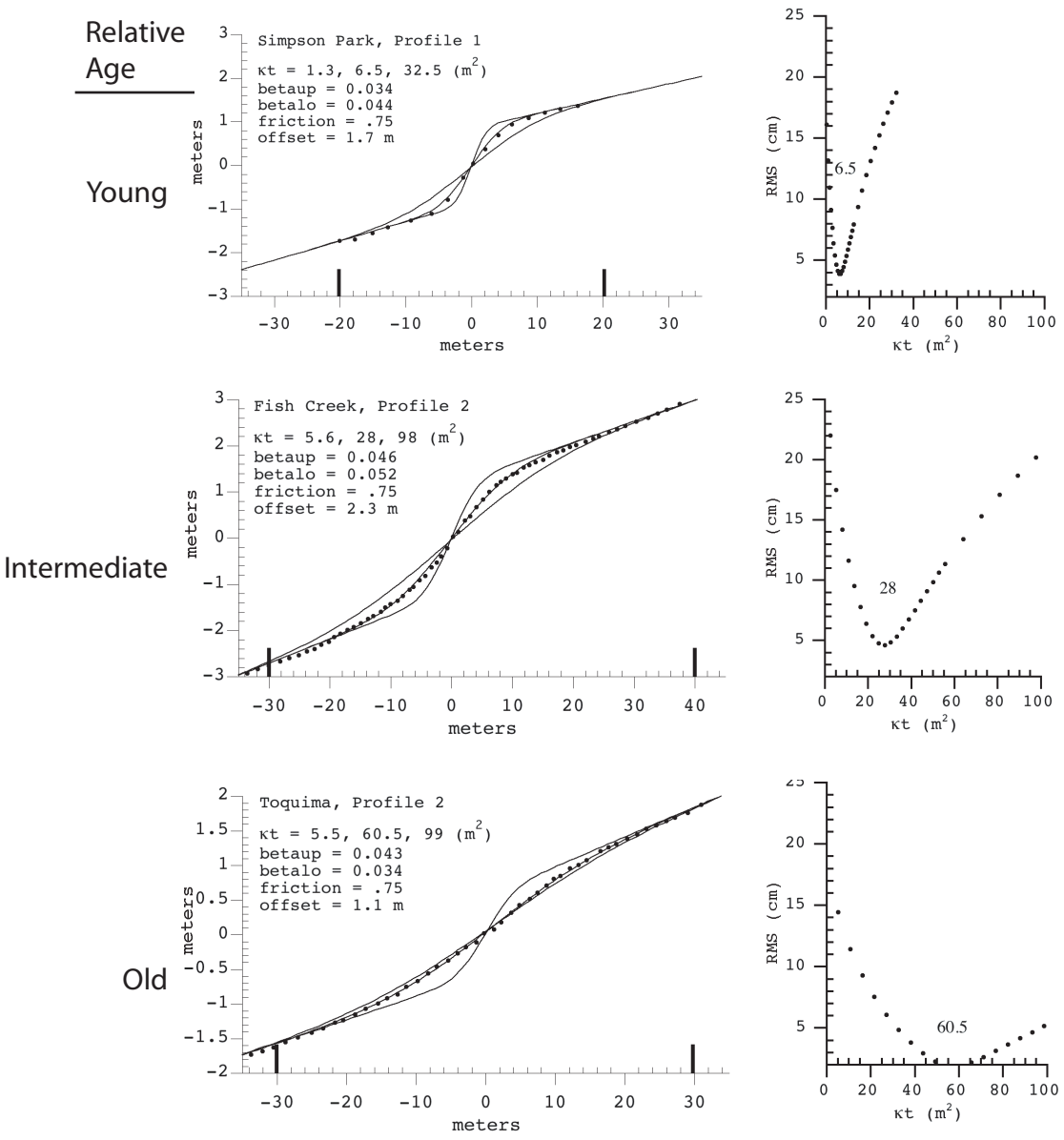

Figure 2. Examples of the approach used to estimate the age of single event fault scarps based on surveyed scarp profiles and diffusion analyses. Examples are shown for scarps of relatively young, intermediate, and old age. Plots of the RMS misfit between observed and synthetic profiles versus a range of kt indicating closeness of fit is shown to right of each profile. A total of 32 scarp profiles were used in the analysis and are archived in Appendix 1. Profiles from multiple event scarps were used only to estimate vertical separation.

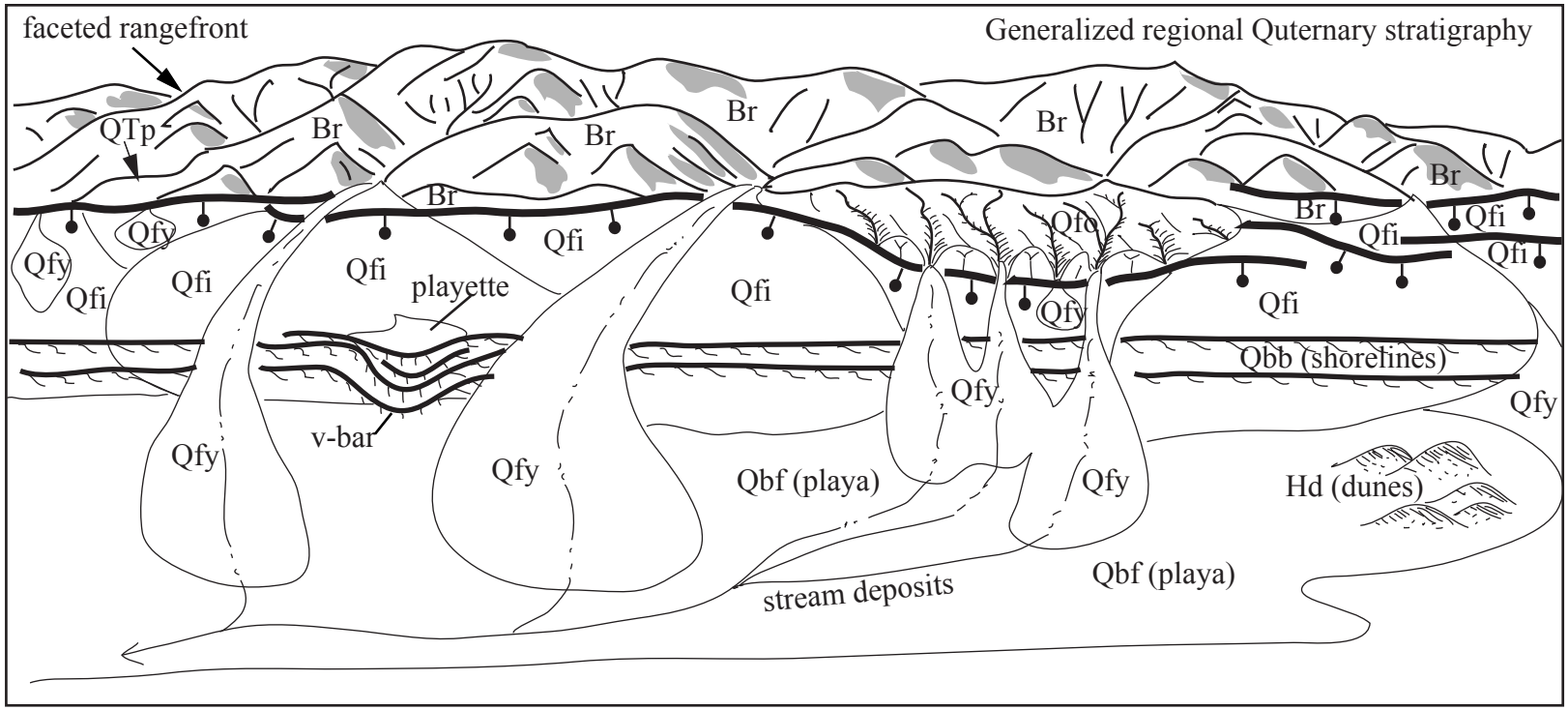

Figure 3. Generalized stratigraphic framework for Quaternary units distributed across the US Highway 50 transect. Stratigraphic units include: Br, bedrock; QTp, Quaternary Tertiary pediment; Qfo, relatively old Quaternary alluvial fan deposits (middle Pleistocene); Qfi, intermediate aged alluvial fan deposits (late Pleistocene); Qfy relatively young Quaternary alluvial fan deposits (latest Pleistocene); Qbf, Quaternary basin fill deposits. Basin fill deposits include: distal alluvial fan, stream, playa (Qbf(p)), lacustrine Qbf(l)), shoreline beach (Qbf(bb)), and Holocene dune (Hd) deposits. Unit abbreviations used in Quaternary strip maps and text. On Quaternary strip maps, thick black lines are faults and thin lines are shoreline features.

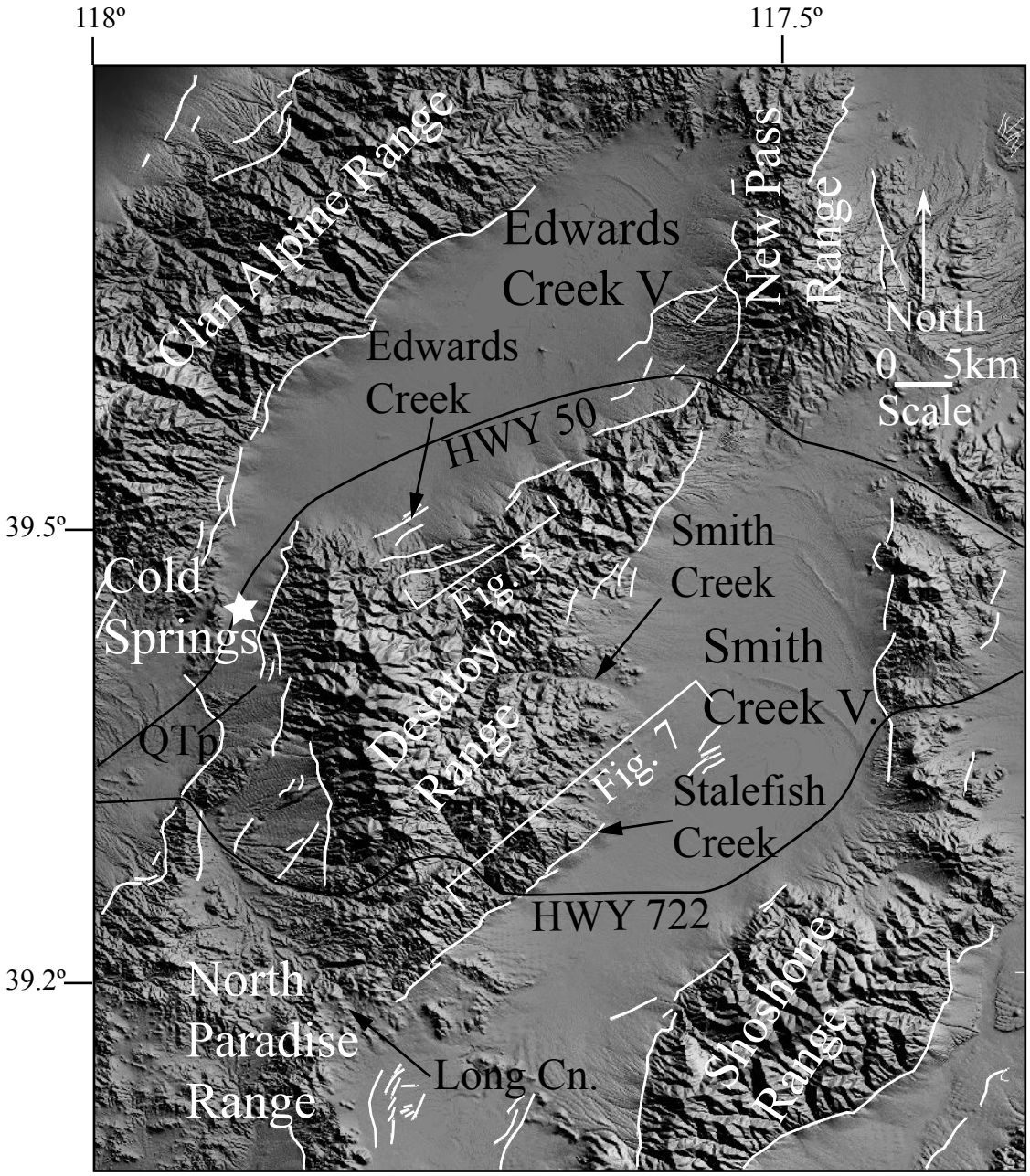

Figure 4. Physiographic map of the Desatoya Range and surrounding region. Previously mapped faults shown in white. Settlement of Cold Springs shown by white star. Highways shown by black lines.

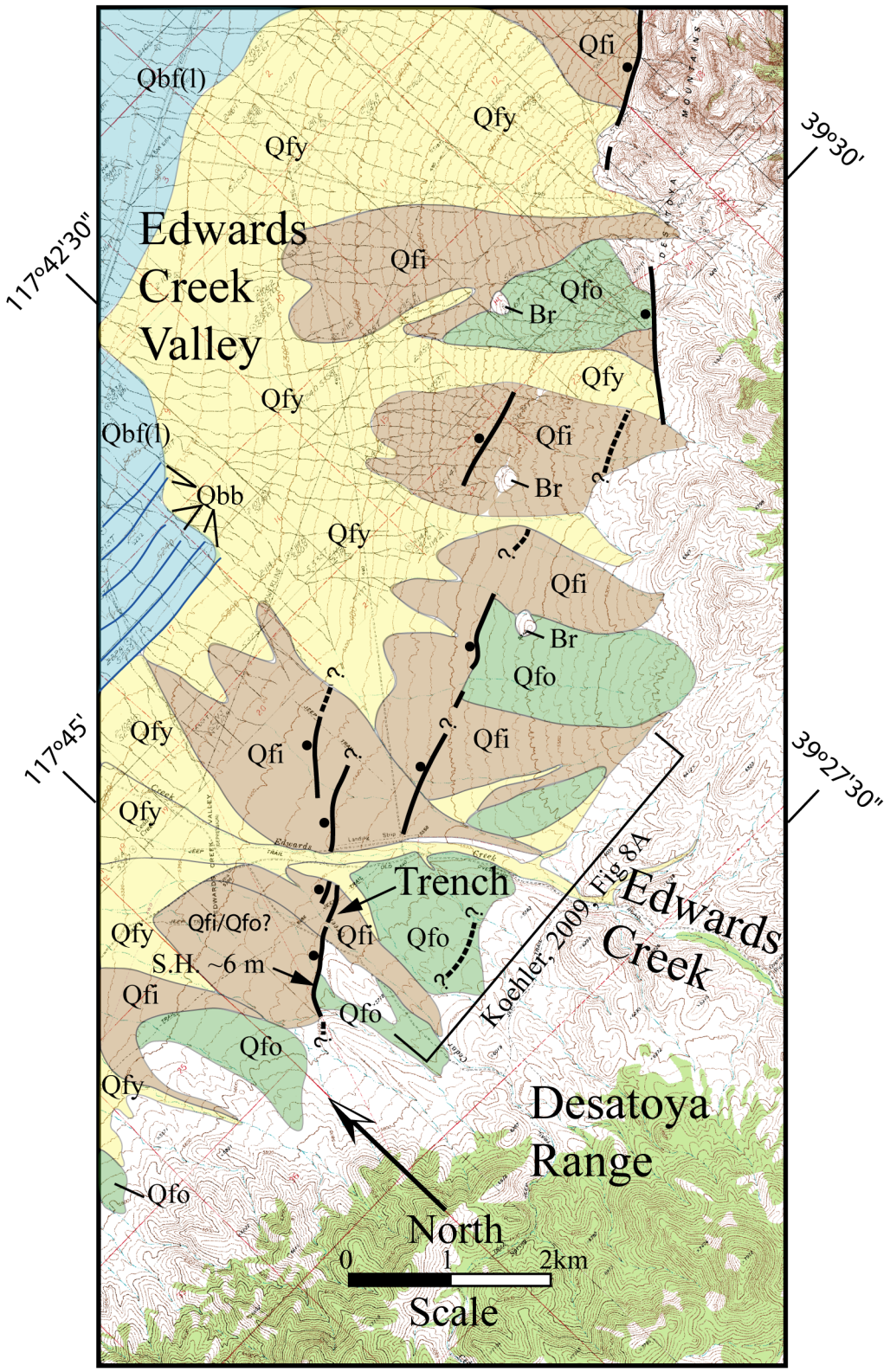

Figure 5. Surficial geologic map along the west side of the Desatoya Range in the vicinity of Edwards Creek, showing traces of the western Desatoya Range fault. Location of air photo, Figure 8A of Koehler (2009) also shown.

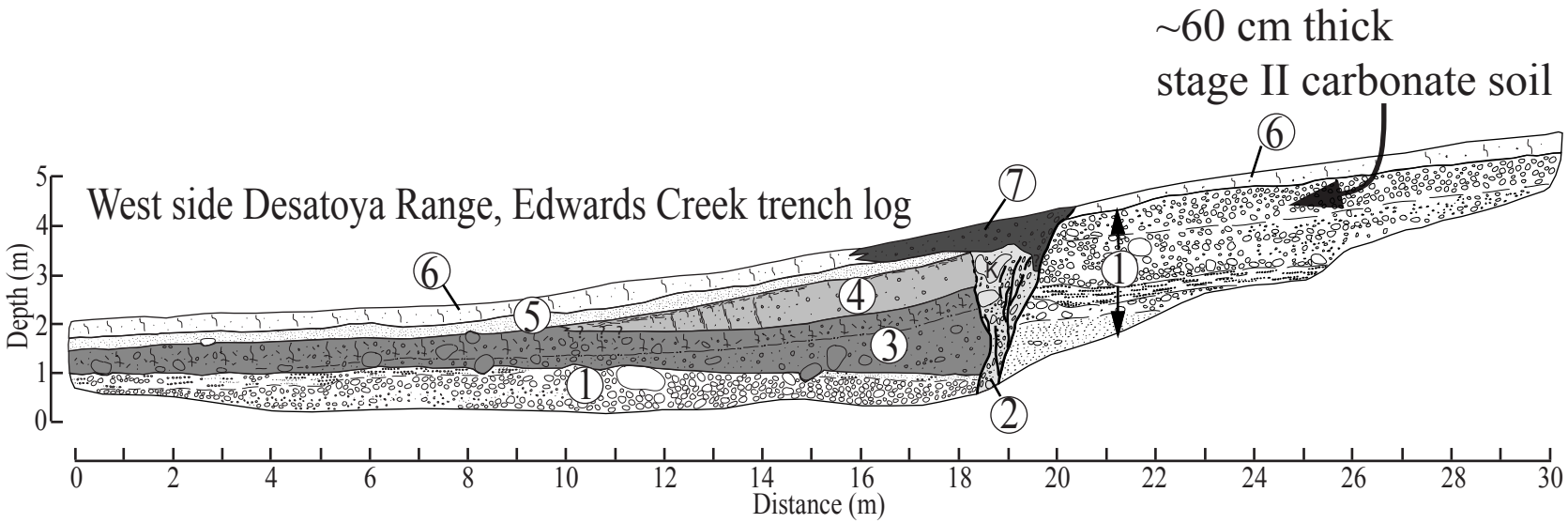

Figure 6. Log of the western Desatoya range fault trench west of Edwards Creek (latitude 39.48246, longitude –116.69593). Most recent earthquake colluvium (Unit 7, black), penultimate colluvium (Unit 4, light gray), oldest earthquake colluvium (Unit 3, dark gray). Unit 1, alluvial fan gravels coarsening upwards from massive, well sorted medium to coarse grained sand, to bedded gravels in a sand matrix, to moderately bedded, clast supported, imbricated, subangular to subrounded cobbles. Upper ~60 cm of Unit 1 is overprinted by a Btk soil horizon with stage II carbonate developmentUnit 2, fissure fill, loose sand, gravel, and vertically aligned cobbles derived from Unit 1. Unit 3, fault scarp derived colluvium, poorly sorted, massive, loamy sand with gravel, upper ~30 cm is a buried Btk soil horizon characterized by clay texture, distinct subangular blocky peds, carbonate nodules and filaments, and 1 cm thick carbonate fillings in cracks. Unit 4, fault scarp derived colluvium, tan, sandy loam with gravel, tapers away from fault zone, upper 20 cm is a buried Btk soil horizon characterized by sandy clay loam texture, subangular blocky peds, olive brown color,m and carbonate stringes trending parallel parallel to upper contact and penetrating cracks through unit. Unit 5, tan, clean sand. Unit 6, Av and Btk soil horizons. Unit 7, fault scarp colluvium, loose, poorly sorted, infills fault zone.

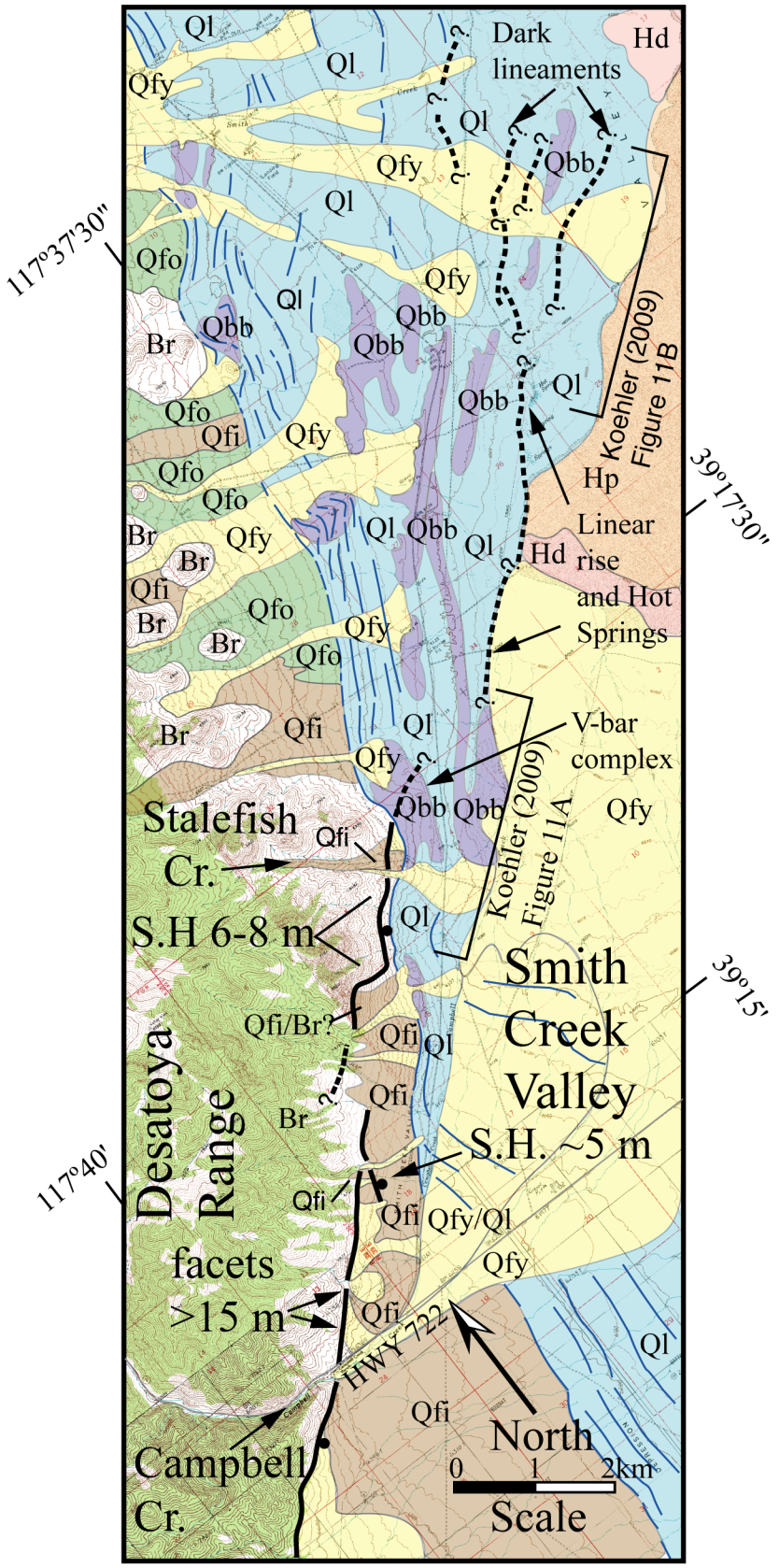

Figure 7. Surficial geologic map showing traces of the eastern Desatoya Range fault and possible projection into young deposits associated with pluvial Lake Desatoya. Locations of air photos, Figures 11A and 11B from Koehler (2009) also shown.

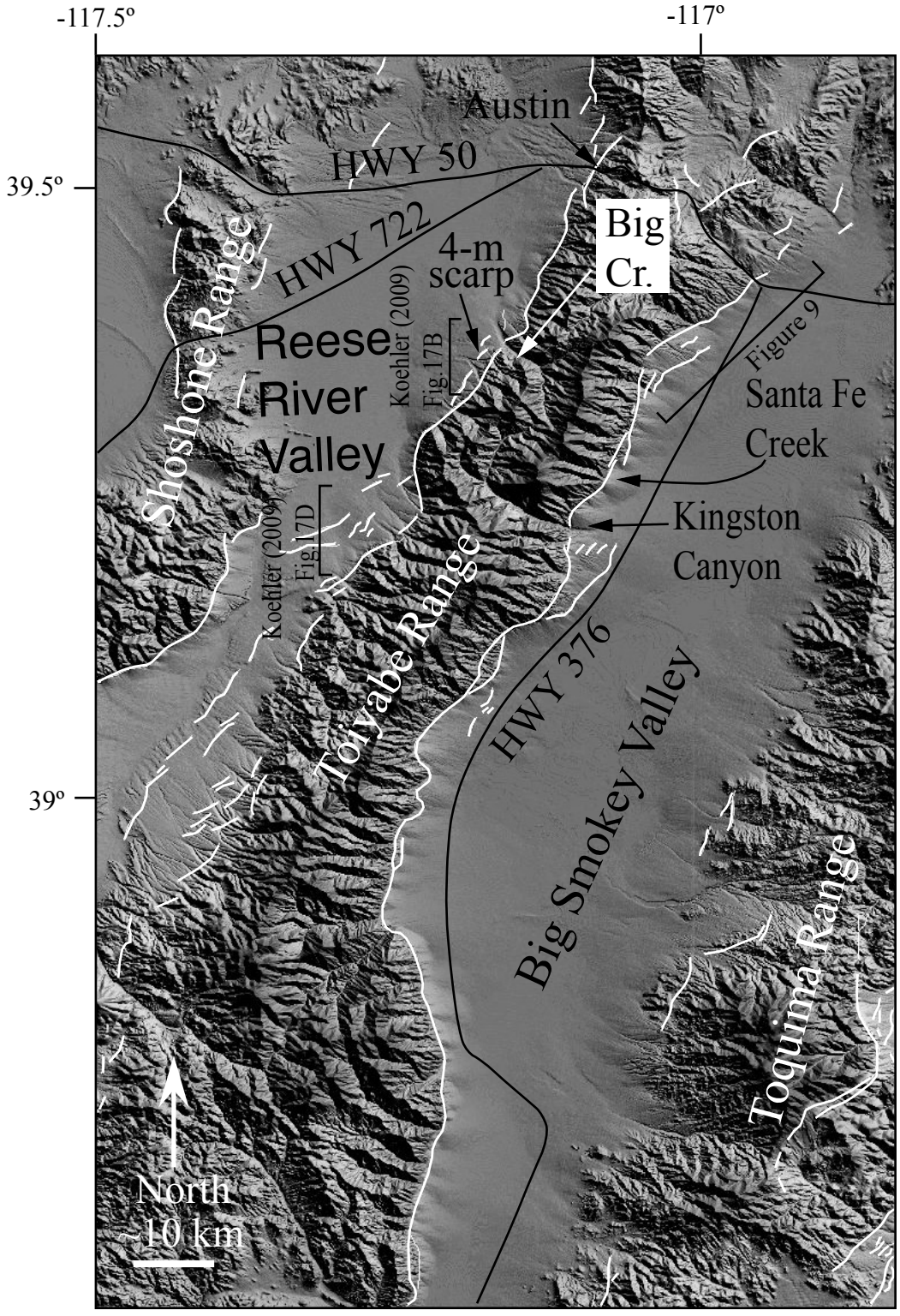

Figure 8. Physiographic map of the Toiyabe Range. Previously mapped faults shown in white. Area of detailed Quaternary mapping shown on Figure 9 is annotated. Location of 4-m-high scarp in Qfi alluvium along the western flank of the range (latitude 39.3477, longitude –117.1727) is also shown.

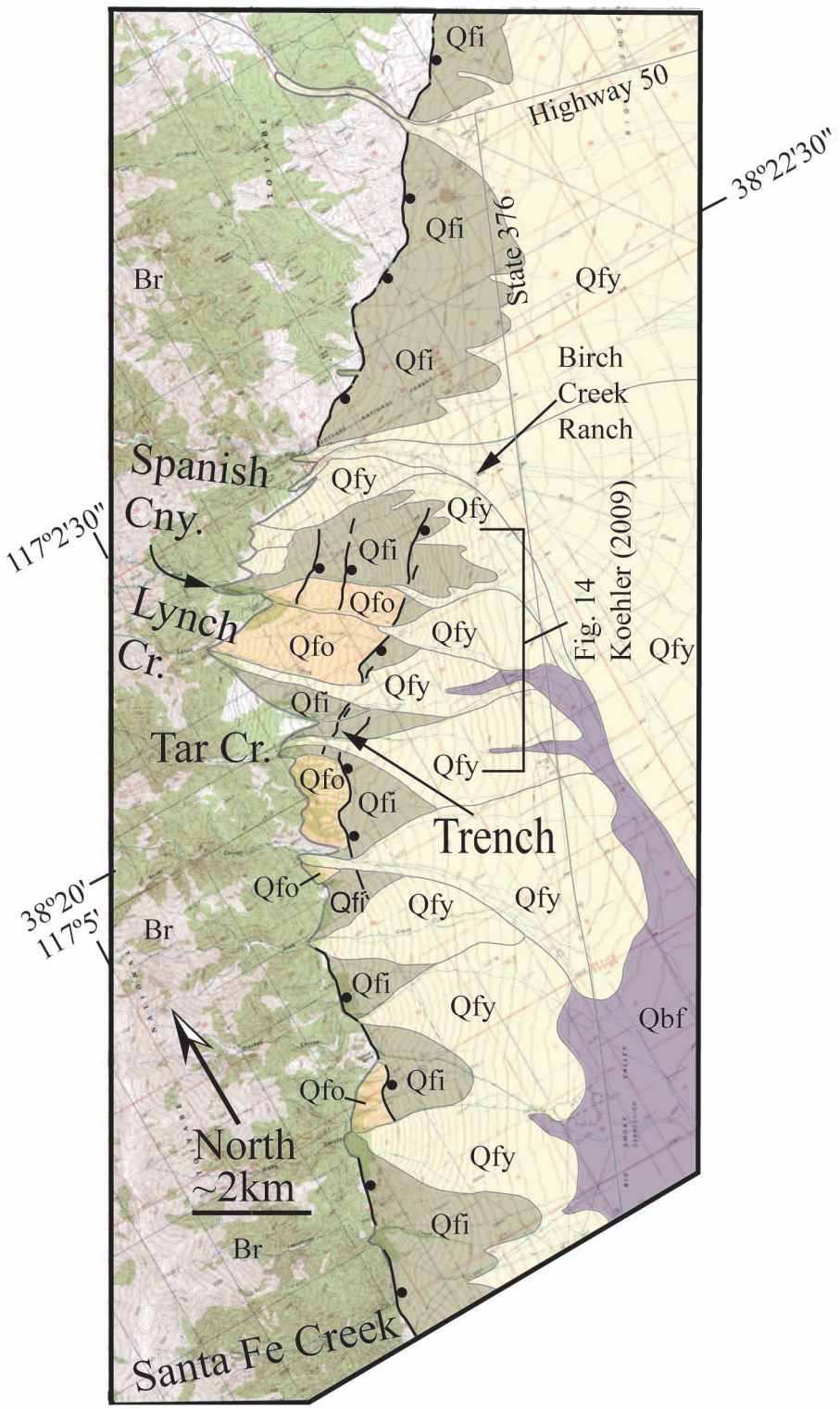

Figure 9. Surficial geologic map showing fault traces of the Eastern Toiyabe Range fault and Quaternary deposits directly south of US Highway 50. Topographic base maps from the Austin, Birch Creek, North Toiyabe Peak, and Simpson Park Canyon USGS 7.5 minute quadrangles. Location of air photo from Figure 14 (Koehler, 2009) is also shown.

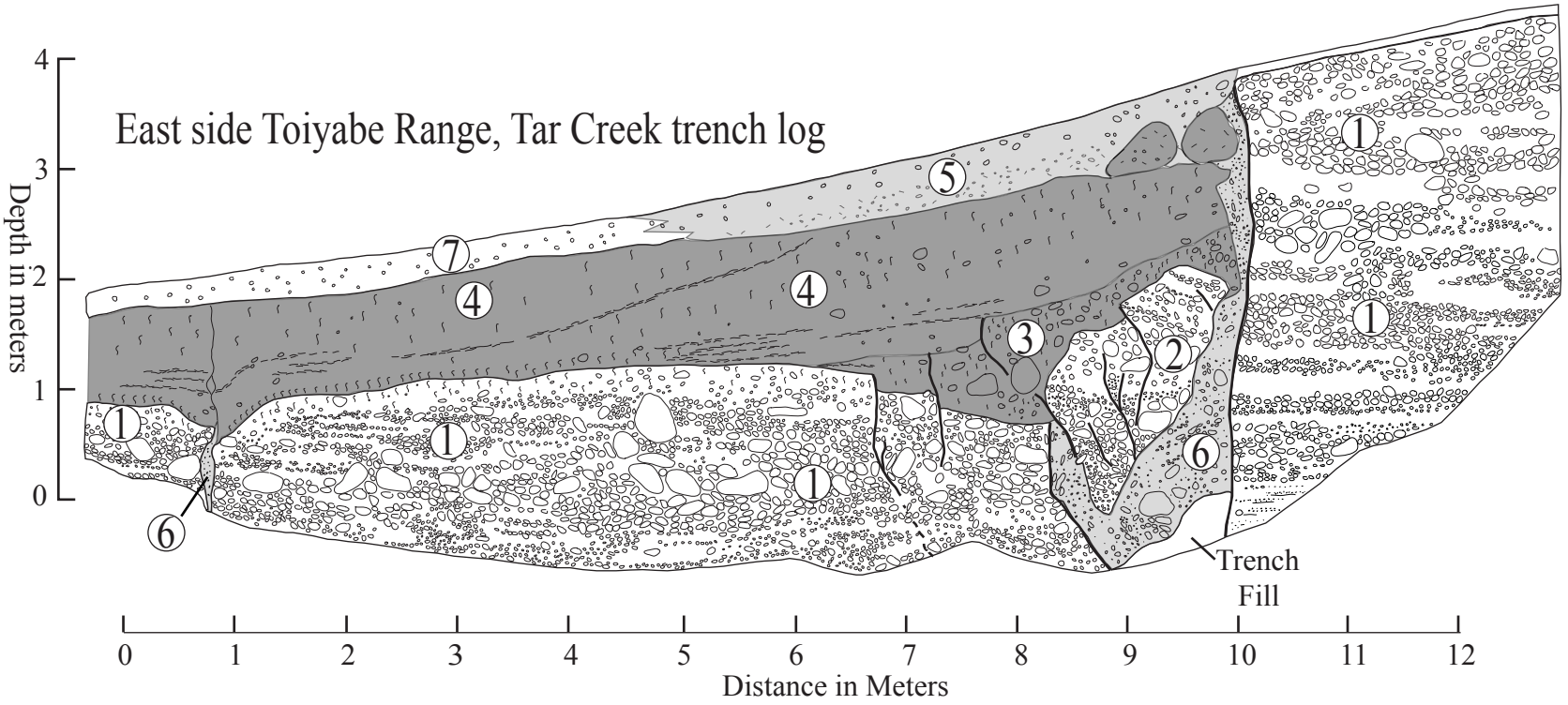

Figure 10. Log of the Tar Creek trench exposure (south wall) located at latitude 39.3352, longitude –117.0219. Unit 1, moderately bedded, imbricated, poorly sorted, subangular to subrounded pebble to boulder clasts in sand matrix. Unit 2, intact block of Unit 1 material backtilted into fault zone. Unit 3, debris facies of penultimate event colluvium (dark gray), unsorted, carbonate coated pebbles and cobbles in a silty sand matrix. Unit 4, wash facies of penultimate event colluvium, massive, carbonate rich, silty sand to sandy silt with trace clasts and is characterized by numerous 1 to 4 cm thick east dipping platy partings of pedogenic carbonate. Unit 5, most recent earthquake colluvium (light gray), loose sand and trace cobbles, thins to east. Unit 6, fissure fill material, loose, unconsolidated, silty sand with randomly oriented clasts. Unit 7, loose surface soil, sandy silt with trace pebbles (Av and Btk horizon of soil profile).

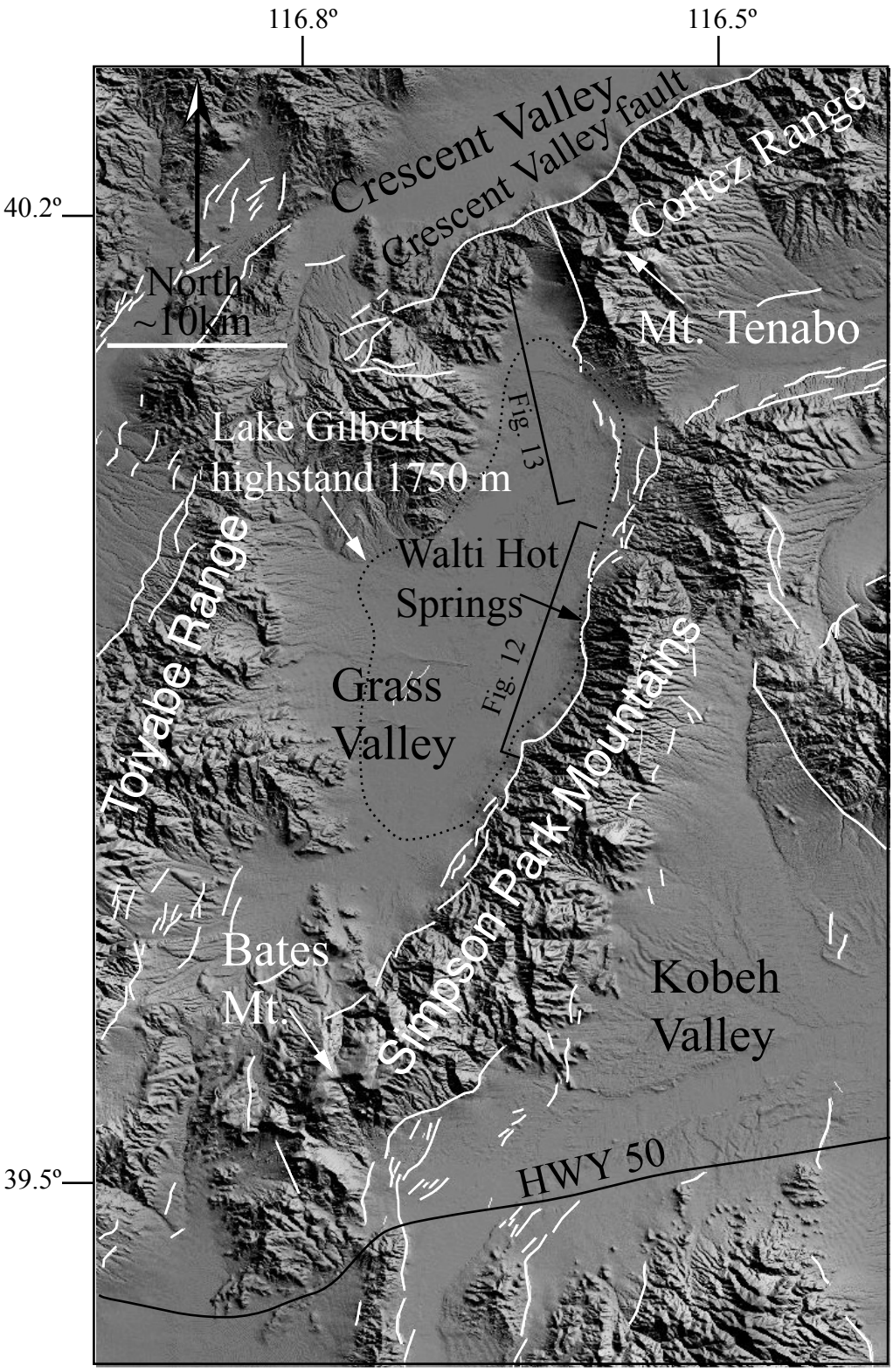

Figure 11. Physiographic map of the Simpson Park Range and Grass Valley. Previously mapped faults shown in white. Approximate outline of pluvial lake Gilbert highstand shown by dotted black line.

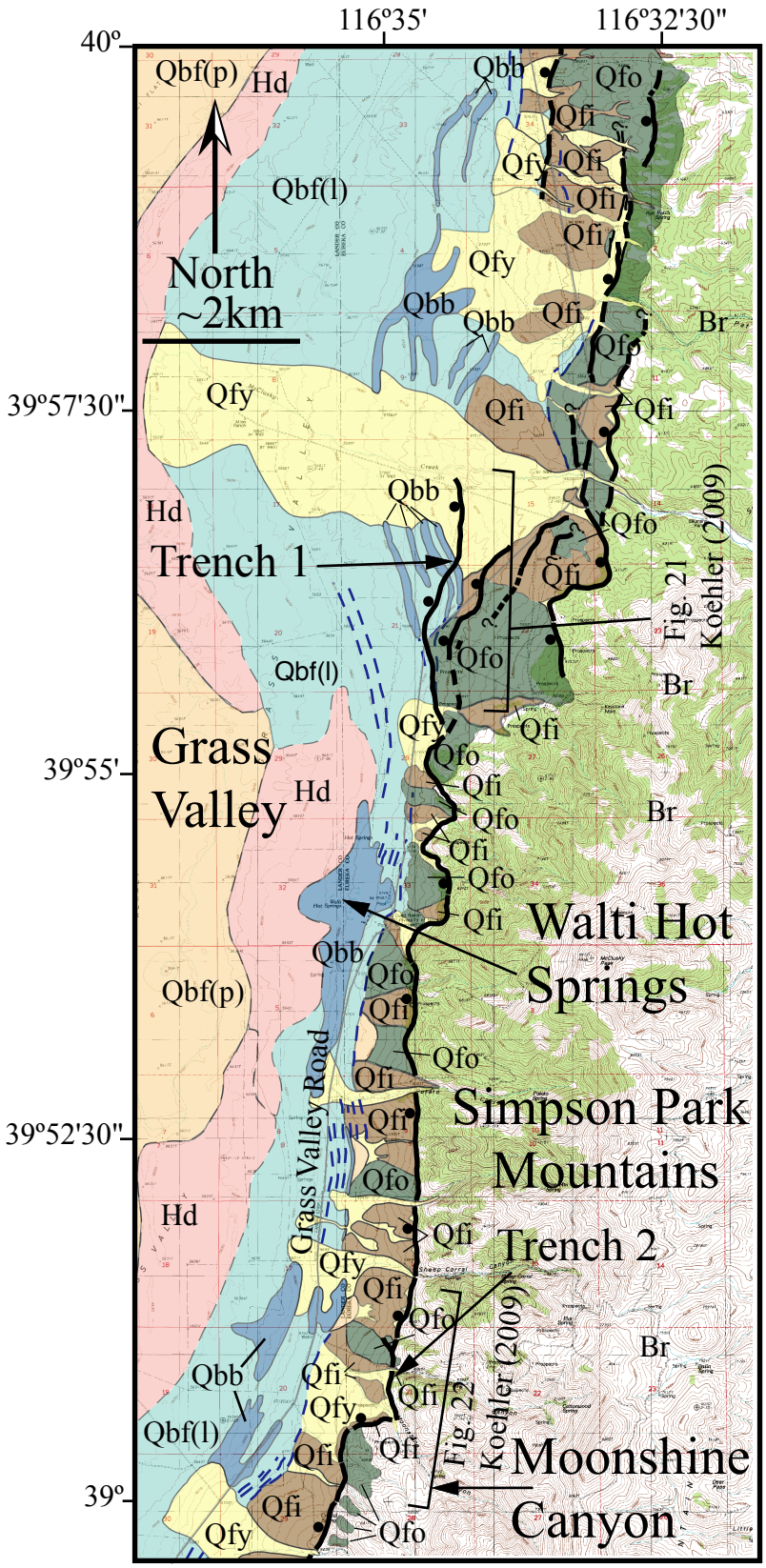

Figure 12. Surficial geologic map of the Simpson Park Mountains fault in the area north of Moonshine Canyon within the Walti Hot Springs and Fagin Mountain USGS 7.5 minute topographic quadrangles. Air photos of trench sites 1 and 2 are archived on Figures 21 and 22 in Koehler (2009).

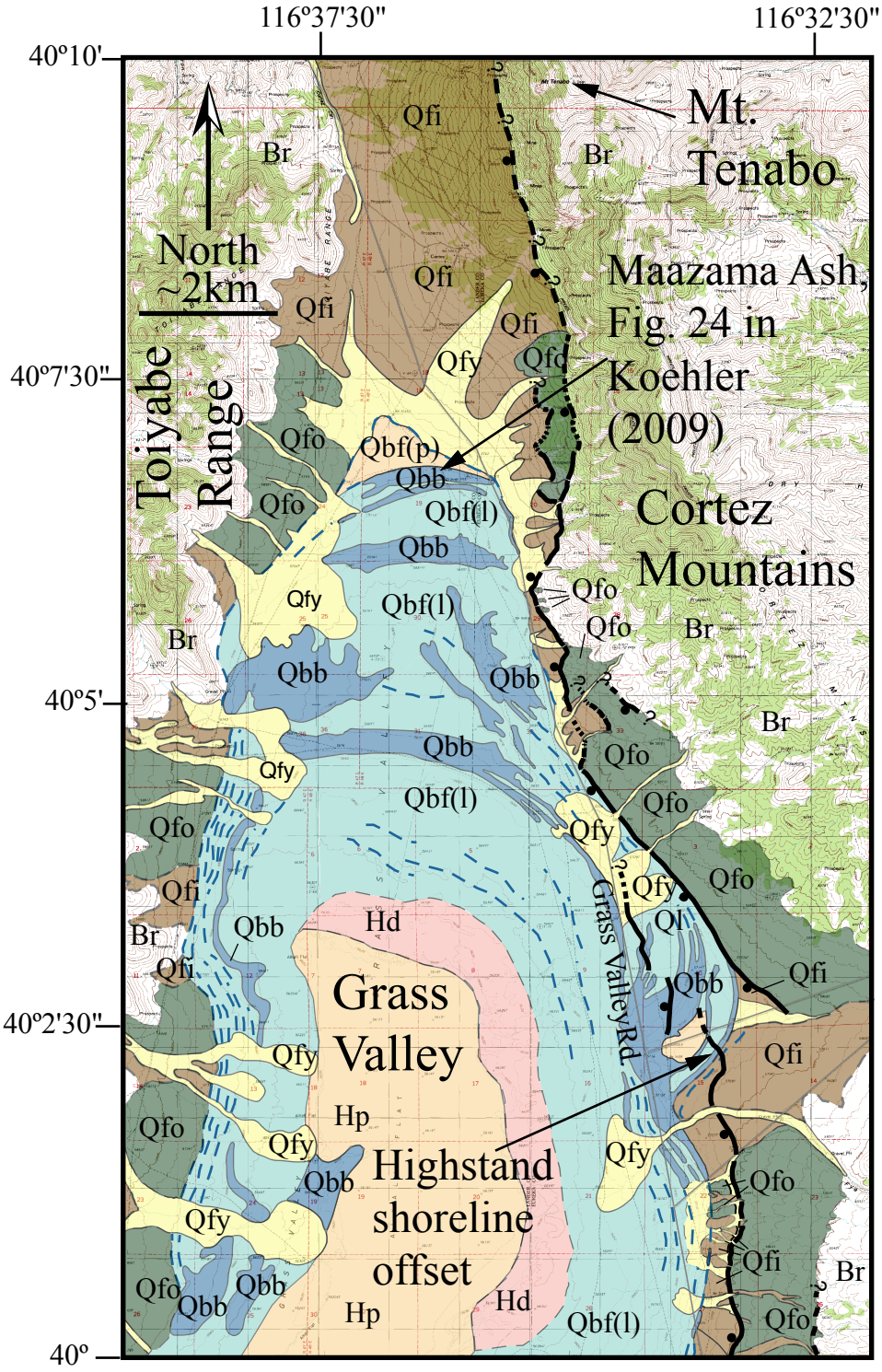

Figure 13. Surficial geologic map of the Simpson Park Mountains fault in the northern part of Grass Valley within the Cortez, Cortez Canyon, Wenban Spring, and Dugout Spring 7.5 minute topographic quadrangles. Location of Maazama ash site (Figure 24 in Koehler, 2009) is also shown.

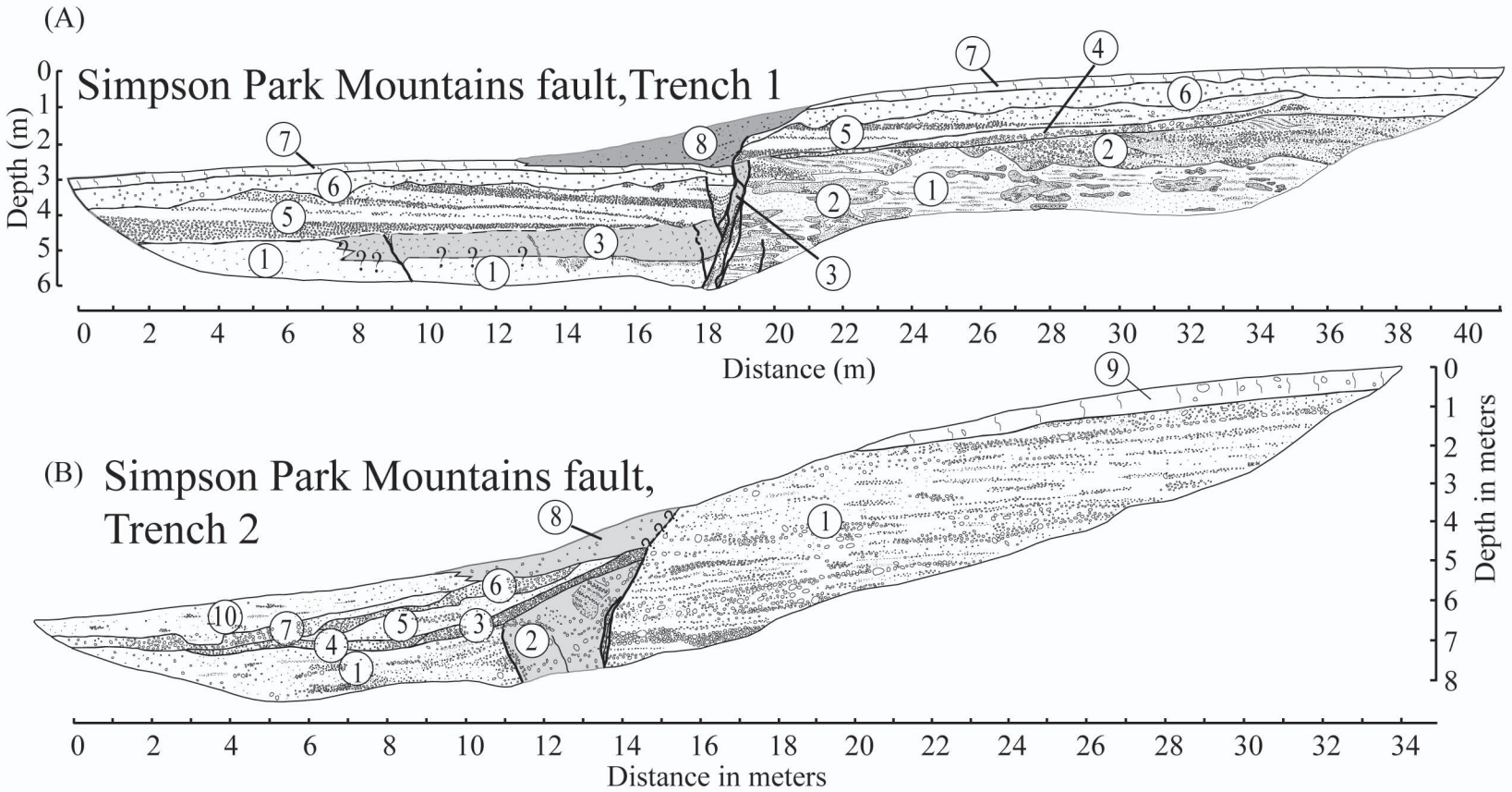

Figure 14. Stratigraphic logs of trench exposures along the Simpson Park Mountains fault. (A) Trench 1 located at latitude 39.94087, longitude –116.57371. Unit 1, laminated sands and silts. Unit 2, thinly bedded, well-sorted sand and gravel channel deposits. Units 1 and 2 may be distal alluvial fan, prograding delta, or nearshore lacustrine deposits. Unit 3, fault scarp colluvium (shaded light gray) dense, sand and silt with trace gravel and stage II carbonate morphology. Unit 4, matrix supported subrounded cobbles. Unit 5, high-energy beach deposit, well sorted, well bedded, backset subrounded to rounded pebbles. Unit 6, sand with gravel Bwk soil horizon with stage 1+ carbonate development. Unit 7, sandy loam A horizon. Unit 8, most recent earthquake colluvium (shaded dark gray), loose, poorly sorted sand and gravel. (B) Trench 2 located at latitude 39.84821, longitude –116.58388. Unit 1, alluvial fan deposits interbedded subrounded to subangular, pebbles to cobbles, poorly sorted, matrix supported, includes lenses of fluvial deposits, moderately sorted, grain supported gravels and sand. Unit 2, graben fill from most recent earthquake (shaded gray), loose unconsolidated sand, gravel, and cobbles, vertically aligned clasts, and intact, backtilted blocks of Unit 1. Unit 3, clast supported subangular gravel possibly raveled off the scarp. Units 4, 5, 6, 7, and 10, sand and gravel alluvial fan deposits. Unit 8, loose, poorly sorted sand and gravel, fault scarp colluvium related to most recent earthquake (shaded gray). Unit 9, weak A and AB soil horizons.

Figure 15. Space time diagram showing late Pleistocene earthquake history across the Great Basin from the Sierra Nevada to the Wasatch Mountains between 38.5° and 40.5° latitude including information from previous studies in Utah and Nevada. The vertical axis is time and the horizontal axis is distance. Horizontal axis is expanded but roughly scaled to the map below. Solid black symbols are earthquakes investigated in this study and open symbols indicate earthquakes studied by others. Circles indicate dated earthquakes, squares indicate number of earthquakes that have occurred since a particular time, stars indicate earthquakes dated by scarp diffusion analyses. Vertical tag lines are numbered the same as faults on map. Tag lines are broken with a diagonal line symbol where events occurred earlier than the time scale. Faults that are the focus of this study and faults studied by others are colored black and grey on the map, respectively. Paleoseismic information for the faults south and north of 40° N latitude are shown on Table 1 and summarized in Wesnousky et al. (2005), respectively. Faults; 1. Genoa, 2. Peavine Peak, 3. Honey Lake, 4, Warm Springs, 5. Pyramid Lake, 6. Shawaves, 7. Bradys, 8. Humboldt, 9. Santa Rosa, 10. Stillwater (east side), 11. Sonoma, 12. East gate, 13. Clan Alpine, 14. Desatoya (west side), 15. Desatoya (east side), 16. Toiyabe (west side), 17. Shoshone, 18. Toiyabe (east side),19. Tuscarora-Malpais, 20. Dry Hills, 21. Cortez, 22. Simpson Park, 23. Toquima south and north (Hickison Summit), 24. Monitor, 25. Antelope, 26. Fish Creek, 27. Diamond (east side), 28. Butte, 29. East Humboldt, 30. Pequops, 31. Egan, 32. Schell Creek, 33. Snake Valley, 34. Deep Creek, 35. Fish Springs, 36. House Range, 37. Crickett Mountains, 38. Drum Mountains, 39. Clear Lake, 40. Stansbury, 41. E. Great Salt Lake, 42. Oquirrh, 43. S. Oquirrh, 44. Little/Scipio Valley, 45. Japanese Valley, 46. & 47. Wasatch. Historic Ruptures (CNSB) shown as rectangular boxes include; A. 1932 M7.2 Cedar Mountain, B. 1954 M7.2 Fairview Peak, C. 1954 M6.8 Dixie Valley/Sand Spring, D. 1954 M6.8/6.6 Rainbow Mtn & Stillwater, E. 1915 M7.7 Pleasant Valley.

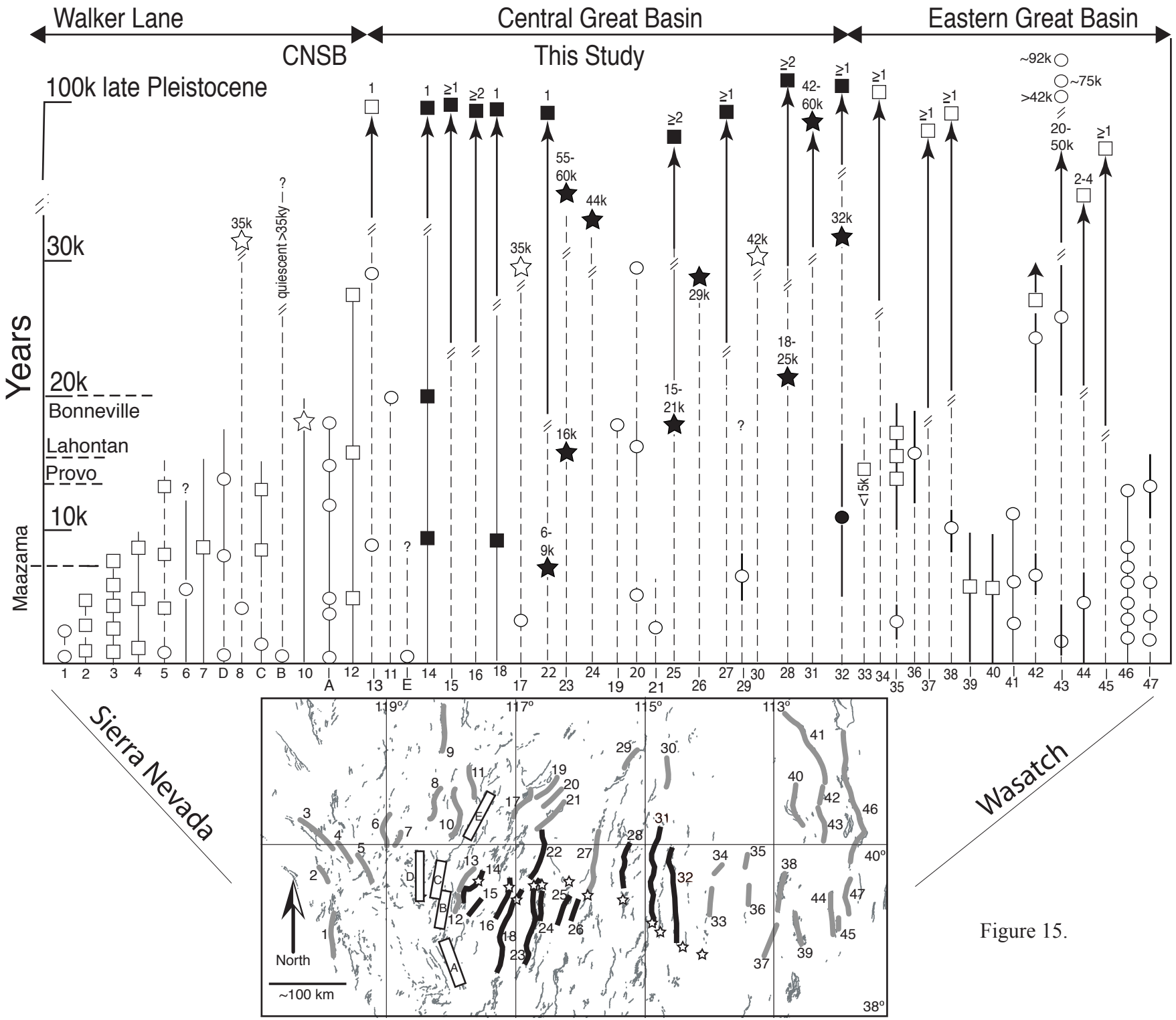
Walker Lane
Central Great Basin
Eastern Great Basin
CNSB
This Study
100k late Pleistocene
30k
20k
Bonneville
Lahontan
Provo
10k
Maazama
Years
35k
quiescent >35ky
55-60k
44k
16k
6-9k
42-60k
32k
29k
42k
18-25k
15-21k
<15k
~92k
~75k
>42k
20-50k
2-4
Sierra Nevada
Wasatch
North
~100 km
119°
117°
115°
113°
40°
38°

Figure 15.

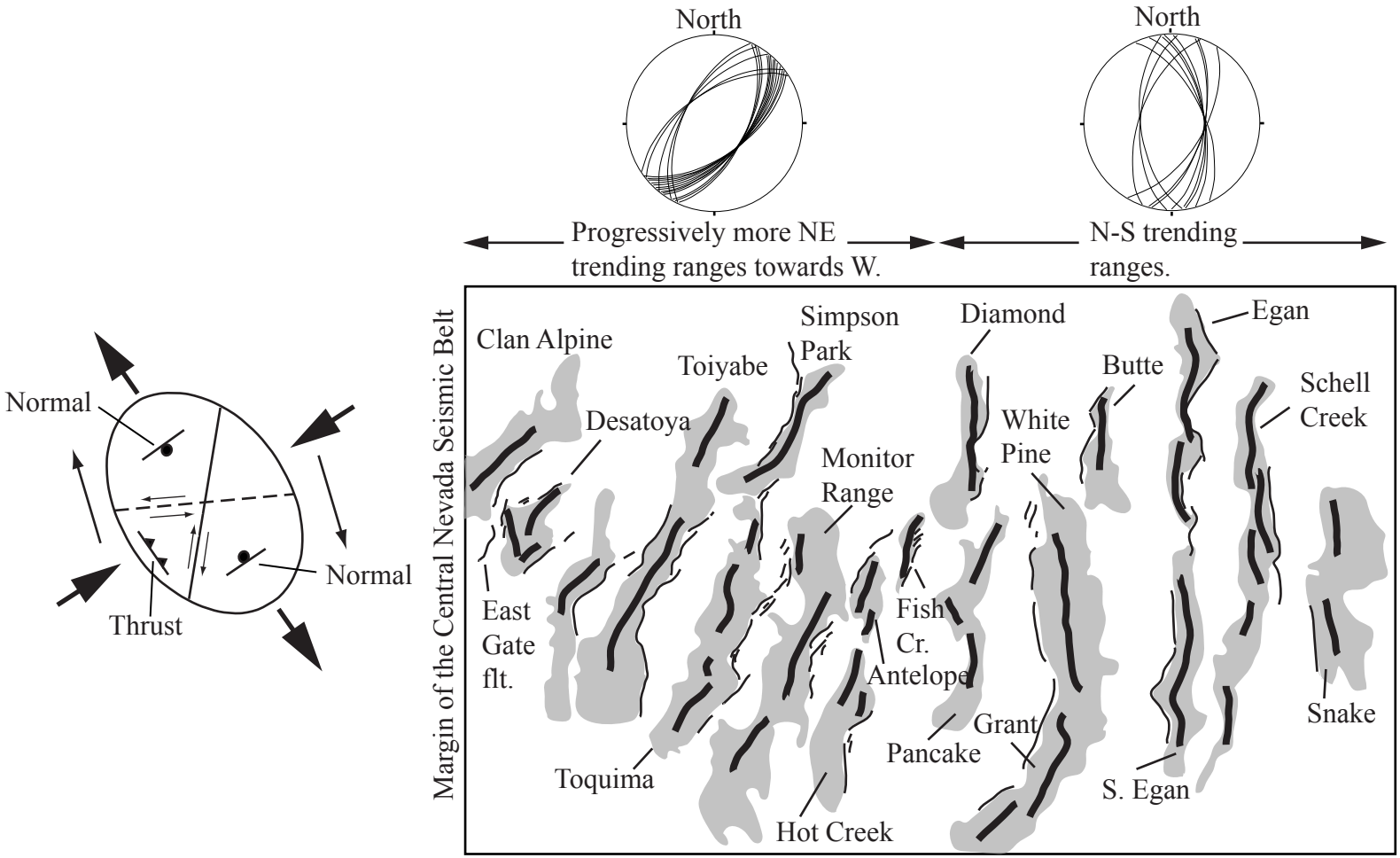

Figure 16. Map of the central Great Basin showing mountain range crests (thick black lines) that are progressively more northeast trending to the west. Gray is the footprint of the mountain ranges. Thin black lines are late Quaternary fault ruptures. Stereo plots of late Quaternary ruptures in alluvium for areas west and east of the Diamond Range are shown above the map and are all plotted with a 600 dip. A strain ellipse approximately oriented with the direction of Pacific/North American relative plate motion shows the favorable orientation for the development of northeast trending normal faults.